

Co-funded by the



DISCO

Grant Agreement: 755443

DELIVERABLE D4.2

Model materials experiments: Dissolution results for modelling input

Dirk Bosbach (FZJ), Christelle Cachoir (SCK•CEN), Christophe Jegou (CEA), Emmi Myllykylä (VTT), Nieves Rodriguez-Villagra (CIEMAT)

Date of issue of this report: **30/06/2020**

Report number of pages: 39

Start date of project: **01/06/2017**

Duration: 48 Months

Project co-funded by the European Commission under the Euratom Research and Training Programme on Nuclear Energy within the Horizon 2020 Framework Programme		
Dissemination Level		
PU	Public	X
PP	Restricted to other programme participants (including the Commission Services)	
RE	Restricted to a group specified by the partners of the Disco project	
CO	Confidential, only for partners of the Disco project	

Table of contents

1	Introduction	3
2	Dissolution results for modelling input	5
2.1	Cr/Al/Gd doped UO₂ model systems.....	5
2.1.1	Results from SCK CEN.....	5
2.1.2	Results from FZJ	14
2.1.3	Results from VTT.....	17
2.1.4	Results from CIEMAT	22
2.2	MOX related model systems	28
2.2.1	Results from CEA	28
3	Concluding perspective.....	35
4	References	36
	Acknowledgement	37
	Appendix	38

1 Introduction

Within the EU DisCo project (www.disco-h2020.eu), experiments on irradiated doped fuels are complemented with dissolution studies using systematically produced and carefully characterized simplified UO_2 -based model materials to understand the effects of the addition of dopants (Cr, Al, Gd) into the fuel matrix on spent nuclear fuel (SNF) dissolution behaviour under repository relevant conditions. These model materials comprise (i) UO_2 reference materials, and (ii) Cr/Al/Gd-doped UO_2 , both, with and without alpha-emitting nuclides such as Pu-238, to address the effects of alpha-radiolysis on the oxidative dissolution of aged SNF after recession of the beta/gamma radiation field in the long-term. Single-effect studies on the dissolution behaviour of the model materials will provide complementary insights and supporting process understanding regarding the performance of modern doped fuels in the repository environment, which cannot be directly obtained from dissolution studies on “real” SNF.

The **main objectives of workpackage (WP) 4** of DisCo are: (1) Understanding matrix corrosion of modern LWR fuels under deep geological repository relevant conditions, and (2) Systematic corrosion studies on Cr/Al/Gd-doped- UO_2 -based and MOX model systems (prepared and characterized in WP2) complementary to SNF corrosion studies in WP3. Special focus will be on the long-term (> 1,000 years) SNF matrix corrosion by using alpha-doped model systems. The experimental programme is intended to overcome the inherent complexity of SNF corrosion and to identify the separate effects of microstructure, doping level, and surface area in support of the spent fuel corrosion studies in WP3. The results will allow for improving the predictive capability of SF corrosion models and reduction of associated uncertainties.

Since the formal start of WP4 in February 2018 a broad range of samples has been studied in a range of experimental conditions. The current status of these systematic studies is compiled in chapter 2 of this report. In general, a set of experimental conditions has been defined in close communication with WP3 in order to allow for an easier comparison between the dissolution experiments performed in WP3 and WP4. Five different chemical compositions for the aqueous solution have been defined: (1) a bicarbonate solution similar to the one used in the First Nuclides project in combination with H_2 atmosphere (reducing, anoxic), (2) young cementitious water in combination with H_2 atmosphere (YCWCa, reducing, anoxic), (3) synthetic CO_x water, (4) natural ground water (with $\text{Fe}(0)$), and (5) bicarbonate and cementitious waters containing H_2O_2 (for accelerated dissolution experiments).

The dissolution behaviour of the model systems has been studied on respective pellets, which were prepared (and characterized) in WP2. One focus was on Cr-doped UO_2 pellets. The preparation of these materials by different groups has provided a variety of samples, which cover a broad range in dopant levels and grain sizes. Since these parameters are not known for irradiated modern fuel pellets, the approach followed here ensures that the envelope of these parameters covers most likely those in “real” SNF.

This report comprises contributions from SCK CEN, FZJ, VTT, CIEMAT, and CEA. The report presents preliminary data and conclusions as of May 2020 and will be updated towards the end of the DisCo project. The main aim of this report is to provide the modelling teams of WP5 with the results of the dissolution experiments on the model systems performed in WP4 in a structured and concise way. For this purpose, an excel spreadsheet was developed by WP5 to allow for an electronic data exchange between the experimentalists of WP4 and the modellers of WP5. The layout of this spreadsheet is depicted in the annex of this report. In the following, the results of the dissolution experiments with model systems are summarised, focusing on a detailed description of the actual leaching conditions and the used experimental setup, the evolution of relevant constituents in solution, and the obtained dissolution rates.

2 Dissolution results for modelling input

2.1 Cr/Al/Gd doped UO₂ model systems

2.1.1 Results from SCK CEN

Static dissolution experiments were performed with depleted UO₂ and Cr-doped UO₂ pellets, either in Young Cementitious Water Light at pH 13.5 (YCWCa-L= cementitious water at pH 13.5 with a Ca concentration lower than the concentration at equilibrium [1]) or in bicarbonate solution at pH 9 (= the solution used also in the project First Nuclides, hence denominated as FIN solution). Table 2.1.1.1 gives the composition of the reference waters. The reference solutions contain a non-negligible concentration of Cr and Zn, especially for the YCWCa-L solution. All tests are performed in an Ar glove box with pO₂ below 10 ppm and pCO₂ below the detection limits. All experimental details (materials, water composition, set-up and conditions) are described in the next paragraphs.

Materials – Four model materials are tested: (depleted) UO₂, Cr-doped (depleted) UO₂, Pu-doped UO₂ and Pu/Cr-doped UO₂. These model materials are synthesised at SCK CEN in collaboration with FZJ within WP2 of this project [2]. Even if the Pu-doped UO₂ production is well known, the production of Cr-doped UO₂ required some development in order to obtain pellets with a density of 95% of the theoretical density, with sufficiently large grains, and with the same specifications as standard fuel (UO₂ reference), i.e. defects, porosity and impurities. The two first years of the project were thus focussed on the development of a production method of the model materials (and on the testing of various methods to control the redox conditions in the experiment). It was concluded that, when the Cr-doped UO₂ is prepared by dry mixing of UO₂ and Cr₂O₃ powders, it is possible to get a grain size close to 50 µm and a more or less homogeneous Cr distribution within the UO₂ matrix (in the grain and at grain boundary). The Pu-doped UO₂ is obtained by a co-precipitation method to achieve a homogeneous distribution of Pu in the UO₂ matrix. The doping level is representative for a fuel age of 10,000 years (~ 18 MBq/g UO₂). The Pu/Cr-doped UO₂ is then synthesised by combining the two previous methods, with first the co-precipitation of Pu in UO₂, followed by dry mixing of Cr₂O₃ and the Pu-doped UO₂ powders. Although FZJ does not recommend the addition of lubricant for the preparation of Cr-doped samples, 0.3 wt% of zinc stearate had to be added at SCK CEN to limit the formation of cracks in the pellets as a result of differences in the press characteristics used at FZJ and at SCK CEN. However, this additive is used also in the industry for the preparation of fuels, so the pellets should be representative of commercial fuel. Even if most of this zinc is volatilised during the sintering process, some traces can be still present within the pellet structure. Therefore, the Zn concentration in solution is also measured during the leaching experiments.

Based on a series of preliminary production tests, a 1600 µg g⁻¹ Cr₂O₃ doping was found to be optimal to reach the requirements [3]. A first set of materials was produced with the characteristics given in Table 2.1.1.2. These depleted UO₂ and Cr-doped UO₂ pellets (Figure 2.1.1.1) were used to start the leaching experiments, although the grain size of the Cr-doped UO₂ (35-50 µm) was slightly less than the target 50 µm. Further optimisation of the speed of

the sintering process, the sieving/crushing and granulometry of the different powders (Cr_2O_3 , UO_2) were attempted to reach a grain size of 50 μm . This optimised procedure will be applied for the preparation of the Pu-doped UO_2 and the Pu/Cr doped UO_2 . In Figure 2.1.1.1 (right), no agglomerates of Cr in the matrix are detected. It was observed, however, that the grain size is smaller near the surface of the Cr-doped UO_2 .

Table 2.1.1.1: Composition of the reference leaching solutions (YCWCa-L and FIN).

mol.L ⁻¹	YCWCa-L	FIN
Na	1.28×10^{-1}	2.07×10^{-2}
K	3.67×10^{-1}	2.33×10^{-5}
Ca	4.43×10^{-4}	5.00×10^{-6}
C	5.08×10^{-4}	9.83×10^{-4}
SO_4^{-2}	1.86×10^{-3}	5.21×10^{-6}
Si	4.32×10^{-5}	3.71×10^{-5}
Cl	$< 8.45 \times 10^{-6}$	1.81×10^{-2}
U	$< 8.40 \times 10^{-10}$	$< 8.40 \times 10^{-10}$
Cr	4.93×10^{-8}	$< 1.35 \times 10^{-8}$
Zn	2.29×10^{-7}	1.17×10^{-7}
pH	13.6	9.1
Eh (MV _{SHE})	177	202

Table 2.1.1.2: Specifications of the depleted UO_2 and Cr-doped UO_2 .

Type of model material	Depl. UO_2	Cr-doped UO_2
Pellet (ϕ mm / h mm)	5.8 / 6	5.8 / 6
TD %	95 ± 1 (95)	95 ± 1 (95)
Cr_2O_3 added ($\mu\text{g}\cdot\text{g}^{-1}$)	0	1600
Grain size (μm)	10 (10)	35- 50 (50)
Geometric Surface area (cm^2)	1.696	1.696
Lubricant*	0.3 wt%	0.3 wt%

Value in brackets corresponds to the target characteristics; * zinc stearate

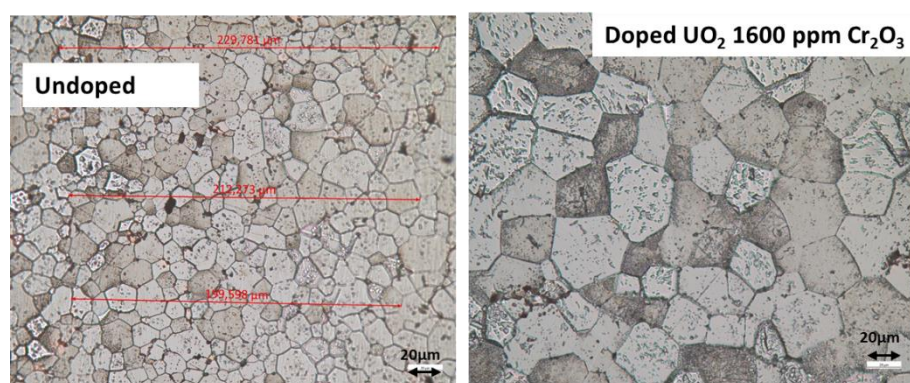


Figure 2.1.1.1: Left - depleted UO_2 (grain size 10 μm), right- Cr-doped UO_2 (grain size 35-50 μm).

Experimental set-up and procedure – Static leaching experiments are carried out in autoclaves with 10 bar H_2 gas in presence of Pt/Pd catalyst to scavenge the oxygen traces inside the autoclaves. The catalyst is placed in the headspace of the autoclaves (and not immersed in the solution), because it should remove traces of atmospheric O_2 without perturbation of the formation of oxidizing species in solution through radiolysis (Figure

2.1.1.2a). The reaction of dissolved H₂ with oxidized species in solution may still be activated by the catalytic properties of the UO₂ surface. No other reducing agent was added to the solution, as preliminary tests showed that this did not improve the redox control [4, 5].

The set-up consists of stainless steel autoclaves with a PEEK insert of 50 ml (Figure 2.1.1.2). The cover of the autoclaves is equipped with two outlet valves. One outlet consists of a short tube stopping immediately under the cover. This is used for gas sampling. The other outlet has a longer tube for the sampling of the solution near the bottom of the solution. A manometer is placed on top of the autoclave to monitor the gas pressure (H₂) during the experiment. Each cell is filled with 30 ml of solution and one pellet of (doped) UO₂ (Table 2.1.1.1), previously washed in 0.01 M NaCl for three weeks. Based on the optimisation of the leaching procedure [4, 5], the experiments are divided into two consecutive steps. A first step consists of a washing period of three to four weeks in 0.01 M NaCl. This washing step is carried out in PE bottles with one pellet per bottle. During the first week the solution is renewed daily while a weekly renewal is done for the weeks thereafter. When the measured U concentration is in the range of the U(IV) solubility ($10^{-8.5 \pm 1}$ M) [6], the leaching experiment is started in one of the reference waters for a period of at least one month. In this period, samples of 2 ml are taken regularly without replenishment, while the autoclaves are put again at 10 bar H₂ pressure.

No annealing of the UO₂ pellets nor pre-leaching in KOH or NaHCO₃ solution is done, as the added-value of these extra treatments was not clearly demonstrated [4, 5]. In order to reduce possible traces of oxygen in the reference solutions, the autoclaves are filled already before the start of the leaching experiment with 30 ml of solution in presence of the Pd/Pt catalyst and placed under 5 bar H₂ pressure during at least one week. The not-filtered U concentrations are measured during the washing and the leaching period while the ultrafiltered U concentrations (< 3.5 nm), corresponding to the dissolved U concentration, are only determined in the leaching step at pH 9 or pH 13.5. We have also determined the not-filtered and ultrafiltered (<3.5 nm) concentrations of Cr and Zn to assess the potential influence of their release on the U behaviour. The Cr concentration is followed as a function of leaching time, while the Zn concentration is measured at the start and at the end of the experiments. All three elements (U, Cr and Zn) are determined by ICP-MS. Sampling was performed after 1, 3, 10, 30 and 72 days of leaching, this corresponds to 22, 24, 31, 51 and 93 days, respectively, including the 21 days of the washing period. The experiments with depleted UO₂ and Cr-doped UO₂ have been started in October 2019.

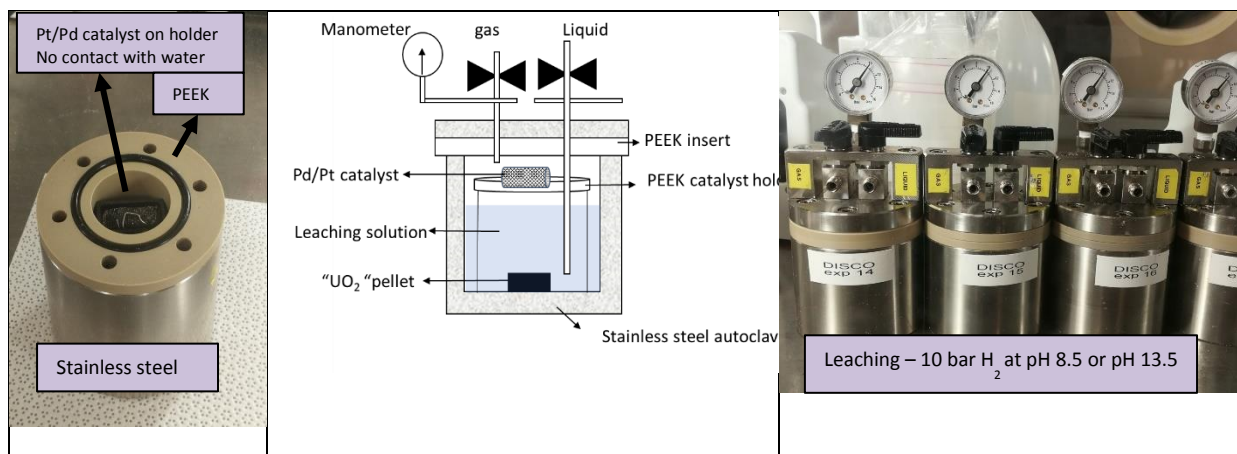


Figure 2.1.1.2: Experimental set-up a: inside the cell, b- schematic drawing and c: autoclaves under 10 bar pressure.

Results and discussion – In the YCWCa-L the pH of the solution remains close to 13.4 ± 0.1 over the leaching period for both depleted UO_2 and Cr-doped UO_2 , while the redox potential is decreasing from -190 to -440 mV/SHE. In the FIN solution, the pH of the leaching solution is more fluctuating and slightly higher (between 9.4 ± 0.3 and 9.8 ± 0.4 for depleted UO_2 and Cr-doped UO_2 , respectively) than the target value of 9. On the contrary, the redox potential behaves similarly as in the YCWCa-L with a decrease from -110 to -350 mV/SHE for whichever the type of UO_2 . The low values of the redox potential in both media suggest that the Pt/Pd catalyst coupled to the H_2 pressure allowed a good scavenging of atmospheric oxygen.

Figure 2.1.1.3 shows the U concentration as a function of time for the depleted UO_2 and the Cr-doped UO_2 during the washing period (0 - 21 days) in 0.01 M NaCl and the leaching period (22-93 days) in YCWCa-L and in FIN solutions. Table 2.1.1.3 gives the measured U concentrations as a function of leaching time for the different experiments.

Uranium concentration during washing period (0 – 21 days)

During the washing in NaCl solution, the U concentration first decreased from $10^{-8} \text{ mol L}^{-1}$ to less than $5.7 \times 10^{-10} \text{ mol L}^{-1}$, this is the detection limit, indicated by the dotted line in Figure 2.1.1.3. In the last samples taken from the NaCl solution (after 21 days), the U concentration slightly increased. It increases somewhat more for the Cr-doped UO_2 ($3.4 \times 10^{-9} \text{ mol L}^{-1}$) than for the depleted UO_2 ($7.5 \times 10^{-10} - 1.5 \times 10^{-9} \text{ mol L}^{-1}$). Although all experimental parameters remained constant (i.e. oxygen in the glove box, temperature), we cannot exclude that oxygen traces in the glove box were responsible for the observed U increase, as the washing step was done in PE bottles that were possibly not fully tight. After 21 days of washing (vertical dotted line in Figure 2.1.1.3), the leaching experiments in the two reference solutions were nevertheless started, as the U concentration was in the range of the U(IV) solubility ($10^{-8.5 \pm 1} \text{ M}$ - red dotted line in Figure 2.1.1.3).

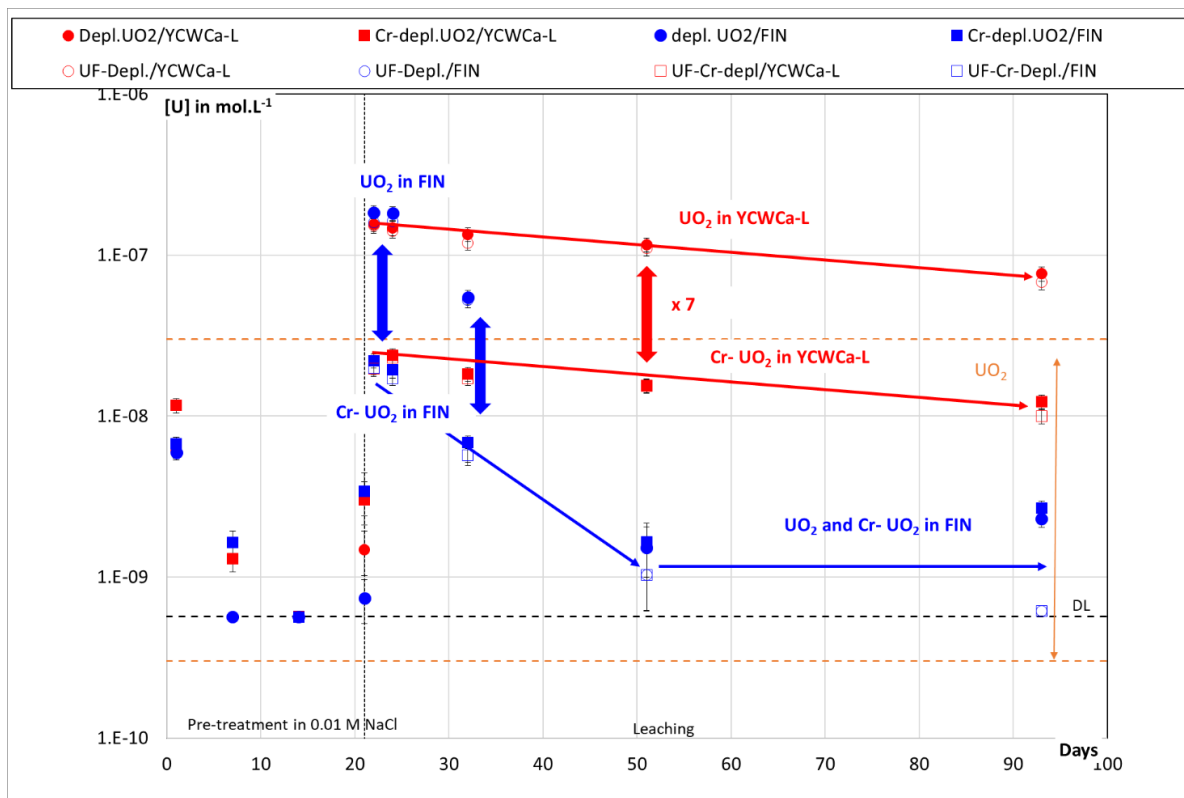


Figure 2.1.1.3: *U concentrations as a function of time for experiments with depleted UO_2 and Cr-doped UO_2 pellets in Young Cementitious water (pH 13.5 - red symbols) and in FIN solution (pH 9 - blue symbols) under 10 bar H_2 . Filled symbols correspond to not-filtered total U concentrations, while open symbols are the ultrafiltered soluble concentrations.*

Uranium concentration during leaching period (21 – 93 days)

At pH 13.5 (YCWCa-L), after a high initial U release, respectively up to 1.6×10^{-7} and $2.2 \times 10^{-8} \text{ mol L}^{-1}$ for depleted UO_2 and Cr-doped UO_2 , the U concentration slightly decreases as a function of time. After 93 days, the U concentration is not yet stabilised and is 7.7×10^{-8} and $1.2 \times 10^{-8} \text{ mol L}^{-1}$ for depleted UO_2 and Cr-doped UO_2 , respectively. As reflected by the U concentrations, the presence of Cr reduces by a factor around 7 the U release for the Cr-doped UO_2 over the entire leaching duration. The ratio colloidal U / total U is small, as shown by the small difference between the total and the ultrafiltered U concentration for both depleted and Cr-doped UO_2 . This difference is mostly $< 10\%$ and corresponds to the uncertainty of the ICP-MS measurements. A high initial U release is also measured at pH 9 (FIN), respectively 1.8×10^{-7} and $2.2 \times 10^{-8} \text{ mol L}^{-1}$ for depleted UO_2 and Cr-doped UO_2 . The U concentration then considerably decreased to stabilize after 51 days around $2.5 \times 10^{-9} \text{ mol.L}^{-1}$ with the a higher ratio of colloidal U / total U, possibly reflecting the over-saturation with a U secondary phase, but the concentration of colloidal U is still small (about 10^{-9} M). Modelling of the experiments will be performed to confirm this hypothesis. Even if during the first 10 days of leaching (up to 31 days in Figure 2.1.1.3), the presence of Cr seems to have a reducing effect on U release similarly as reported in YCWCa-L, this effect disappears with time. After 93 days, the total U concentration close to $2.5 \times 10^{-9} \text{ mol L}^{-1}$ and the soluble U concentration $< 6.2 \times 10^{-10} \text{ mol L}^{-1}$ are identical for the depleted and Cr-doped UO_2 .

Table 2.1.1.3: U concentration in mol L⁻¹ measured after 22, 24, 31, 51 and 93 days for the experiments with depleted UO₂ and Cr-doped UO₂ pellets in Young Cementitious water (pH 13.5) and in FIN solution (pH 9) under 10 bar H₂.

Day	YCWCa-L				FIN			
	Depleted UO ₂		Cr-doped UO ₂		Depleted UO ₂		Cr-doped UO ₂	
	[U] _{Total} mol.L ⁻¹	[U] _{soluble} mol.L ⁻¹						
22	1.6 ± 0.2 x10 ⁻⁷	1.5 ± 0.2 x10 ⁻⁷	2.2 ± 0.2 x10 ⁻⁸	2 ± 0.2 x10 ⁻⁸	1.8 ± 0.2 x10 ⁻⁷	1.6 ± 0.2 x10 ⁻⁷	2.2 ± 0.2 x10 ⁻⁸	2 ± 0.2 x10 ⁻⁸
24	1.5 ± 0.2 x10 ⁻⁷	1.4 ± 0.1 x10 ⁻⁷	2.4 ± 0.2 x10 ⁻⁸	2.3 ± 0.2 x10 ⁻⁸	1.8 ± 0.2 x10 ⁻⁷	1.6 ± 0.2 x10 ⁻⁷	1.9 ± 0.2 x10 ⁻⁸	1.7 ± 0.2 x10 ⁻⁸
31	1.3 ± 0.1 x10 ⁻⁷	1.2 ± 0.1 x10 ⁻⁷	1.8 ± 0.2 x10 ⁻⁸	1.7 ± 0.2 x10 ⁻⁸	5.4 ± 0.6 x10 ⁻⁸	5.2 ± 0.6 x10 ⁻⁸	6.8 ± 0.7 x10 ⁻⁹	5.7 ± 0.6 x10 ⁻⁹
51	1.2 ± 0.1 x10 ⁻⁷	1.1 ± 0.1 x10 ⁻⁷	1.6 ± 0.1 x10 ⁻⁸	1.5 ± 0.1 x10 ⁻⁸	1.5 ± 0.5 x10 ⁻⁹	1 ± 0.4 x10 ⁻⁹	1.6 ± 0.5 x10 ⁻⁹	1 ± 0.4 x10 ⁻⁹
93	7.7 ± 0.8 x10 ⁻⁸	6.8 ± 0.7 x10 ⁻⁸	1.2 ± 0.1 x10 ⁻⁸	1 ± 0.1 x10 ⁻⁸	2.3 ± 0.3 x10 ⁻⁹	< 6.1 x10 ⁻¹⁰	2.7 ± 0.3 x10 ⁻⁹	< 6.2 x10 ⁻¹⁰

Between 1 and 3 days of leaching (21- 24 days in Figure 2.1.1.3), the U concentration seems constant and equivalent for the two reference solutions. In this stage, there is no clear effect of pH or the complexing agent (OH⁻ or CO₃²⁻) on the U release. The U concentrations are, however, much lower for the Cr-doped UO₂ than for the depleted UO₂: we can clearly distinguish a reducing effect of Cr on the U concentration by a factor 7- 8. A fast initial dissolution rate has been determined for the depleted UO₂ at 4.6 ± 0.5 (YCWCa-L) and 5.4 ± 0.5 mg m⁻² d⁻¹ (FIN), while somewhat lower initial dissolution rates were determined for the Cr-doped UO₂ at 0.7 ± 0.1 (YCWCa-L) and 0.6 ± 0.1 mg m⁻² d⁻¹ (FIN). These values support the lowering effect of Cr on the UO₂ dissolution rate. The nature of the complexing agent does not play any role on this initial release.

After this short initial period (after 24 days in Figure 2.1.1.3), no meaningful dissolution rate can be determined as the U concentrations are decreasing for all experiments. However depending on the type of solution, the U release has different behaviours. In YCWCa-L, even if the U concentrations are slightly decreasing by a factor of about 2 between 24 and 93 days for the depleted and Cr-doped UO₂, the Cr effect on U release (the factor 7 difference between depleted and Cr-doped UO₂) remains constant over time. This suggests a continuous driving effect of the OH⁻ on the Cr and U release. In FIN solution, the U concentrations decrease much faster. Moreover, they decrease faster for the depleted UO₂ than for the Cr-doped UO₂. Whereas the Cr-doping decreased the U concentration by a factor 7 to 3 in the first 12 days of leaching (21 - 32 days in Figure 2.1.1.3), the longer term concentrations are thus the same with and without Cr, suggesting a temporary effect of Cr in FIN solution, in the tested reducing conditions.

Several hypotheses can be proposed to explain the lower U concentrations for the Cr-doped UO₂ in YCWCa-L (over the entire test duration) and in FIN (before 51 days). The Cr-doped UO₂ could be less sensitive to oxidation by the exposure to traces of oxygen at the start of the leach test. Secondly, the catalytic properties of the UO₂ surface could be enhanced by the Cr

in the UO_2 , thus making the H_2 more reactive towards oxidizing or oxidized species. Thirdly, the surface of the UO_2 might get covered by precipitating Cr. This would lower the further U release as observed for the Cr-doped UO_2 in both media (Figure 2.1.1.3). Before drawing robust conclusions, these hypotheses need to be confirmed by the surface analysis of the leached materials and also tested by modelling calculations.

Cr concentration

The Cr concentrations are mostly close to the detection limit of the ICP-MS (i.e. from 1 to $8 \times 10^{-8} \text{ mol L}^{-1}$) and close to the background concentration of the reference solutions of 5×10^{-8} and $< 1.4 \times 10^{-8} \text{ mol L}^{-1}$ for YCWCa-L and FIN solutions, respectively. Taking into account the uncertainties on the concentration and the fluctuations of the detection limit of the ICP-MS, a small Cr release can nevertheless be discerned for the Cr-doped UO_2 , especially for the YCWCa-L while no Cr release is observed for the undoped UO_2 , as expected (Figure 2.1.1.4). We focus the further discussion on the Cr-doped UO_2 . At pH 13.5 (YCWCa-L), the total Cr concentration is in the range $5 \times 10^{-8} - 1.9 \times 10^{-7} \text{ mol L}^{-1}$, whereas the soluble Cr concentration is close to $5 \times 10^{-8} \text{ mol L}^{-1}$, which also corresponds to the background concentration of the reference solution. At pH 9 (FIN), the Cr concentrations are lower than at pH 13.5. The total Cr concentration is in the range 8×10^{-8} to $3 \times 10^{-8} \text{ mol L}^{-1}$, while the soluble Cr concentration is around $3 \times 10^{-8} \text{ mol L}^{-1}$.

The doping level of 1600 ppm Cr_2O_3 for the Cr-doped UO_2 would correspond to a Cr concentration in solution close to $4 \times 10^{-5} \text{ mol L}^{-1}$ if all Cr in the pellets would be dissolved. Based on the measured concentrations, we can thus conclude that a very small Cr fraction of 0.2 and 0.5% is released in FIN and YCWCa-L, respectively. We can nevertheless notice that this Cr release fraction is much higher than the released U fraction of 0.0003% for the both solutions, suggesting that Cr could be present in the accessible part of the materials and that the release is promoted at high pH. Furthermore, the constant soluble concentration suggests a Cr phase(s) controlling the concentrations in solution. This assumption is also supported by the presence of colloids highlighted by the difference between the soluble and total Cr concentrations. This observation is valid for both of the reference solutions. Modelling of the experiments might support this hypothesis. The slightly higher soluble concentration in YCWCa-L than in FIN suggests that the Cr release is (slightly) enhanced at high pH.

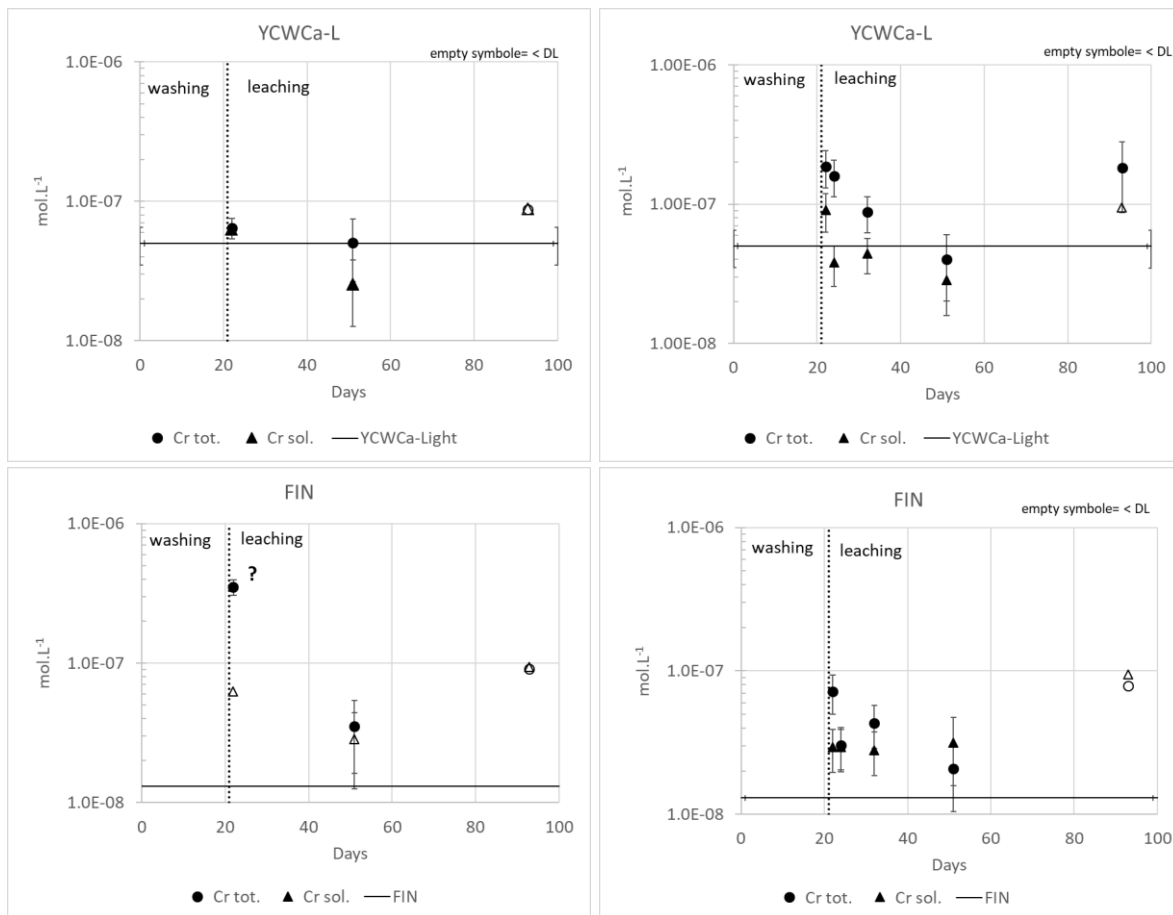


Figure 2.1.1.4: Cr concentrations as function of time for experiments under 10 bar H_2 with depleted UO_2 pellet (left column) and Cr-doped UO_2 pellet (right column) in Young Cementitious water (pH 13.5 - upper graphs) and in FIN water (pH 9 - lower graphs). The horizontal line shows the background concentration. The open symbols are for concentrations below detection limit.

Zn concentration

A clear increase of Zn concentration compared to the background in the reference solutions (Table 2.1.1.1) is observed for both depleted UO_2 and Cr-doped UO_2 in both solutions (Figure 2.1.1.5). The measured concentration appears more or less constant and seems equivalent for the undoped and doped UO_2 leached in the same reference solution. This shows that the Zn stearate, used as lubricant, was not fully volatilized during the sintering process of the pellets and can thus be released during the leaching experiment. However, no interaction of Zn with U and Cr is expected.

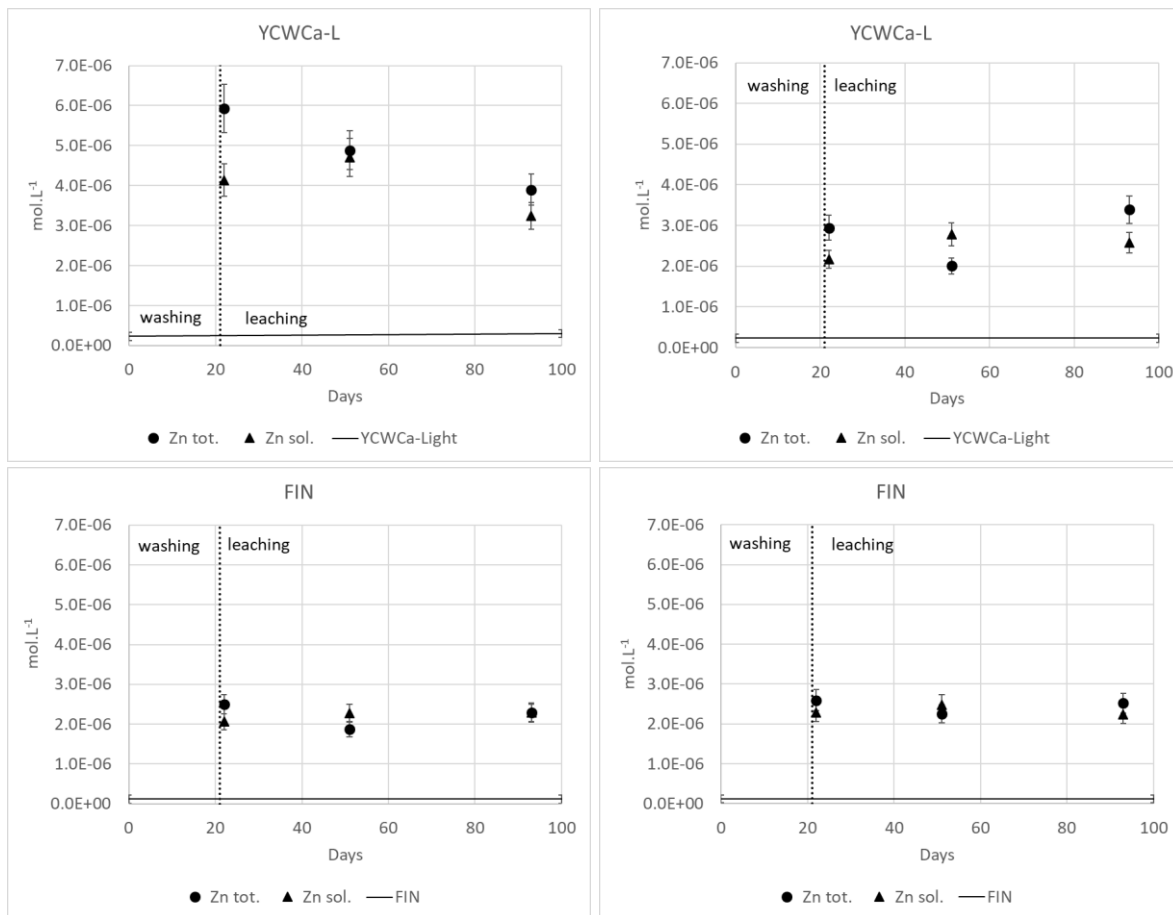


Figure 2.1.1.5: Zn concentrations as function of time for experiments under 10 bar H_2 with depleted UO_2 pellet (left column) and Cr-doped UO_2 pellet (right column) in Young Cementitious water (pH 13.5 - upper graphs) and in FIN water (pH 9 - lower graphs). The horizontal line shows the background concentration.

Conclusions – In this first phase of the leaching experiments of model UO_2 by SCK CEN in the framework of the DisCo project, static leaching tests with depleted UO_2 and Cr-doped UO_2 pellet were performed in autoclaves in the two reference solutions YCWCa-L and FIN under 10 bar H_2 pressure and in presence of Pt/Pd catalyst to scavenge the oxygen present in the autoclave atmosphere. After a fast initial release independent on type of solution, the results demonstrated a promoted U release in cementitious solution compared to bicarbonate water for both kinds of fuels. However, while a reducing effect of Cr on U release is observed continuously in cementitious conditions, this effect seems to be temporary in bicarbonate conditions. Several hypotheses are forwarded to explain these observations, but they need to be supported by future surface analyses and modelling calculations.

2.1.2 Results from FZJ

In the frame of WP4 new accelerated dissolution experiments were carried out in previously degassed bicarbonate solutions (NaHCO_3 , 10 mmol/L) representing groundwater, using hydrogen peroxide (H_2O_2 , 2.25 mmol/L) to mimic the oxidative radiolytic dissolution of UO_2 . UO_2 model materials with and without Cr doping synthesised in the framework of WP2, as well as one commercial available Cr-doped pellet (AREVA) were used for these experiments. To achieve anoxic conditions the solutions were flushed with argon during the complete experimental run time. The experimental setup, developed at FZJ for these dissolution experiments is shown in Figure 2.1.2.1, aimed in particular at:

- maintaining the pellets completely covered with test solution throughout the whole dissolution experiments,
- allowing easy sampling of test solution and permanent flushing of the vessels with argon,
- providing constant conditions avoiding H_2O_2 degradation during the experiments, and
- controlling the experimental temperature.

The setup allowed for the accomplishment of 11 dissolution experiments in parallel. The sample vessels were placed in a massive aluminium block equipped with a water conduit connected to a thermostat for temperature control. Plasticine gaskets were used to close the contact between the vessels and aluminium block and to ensure the light tightness of the vessels. In all experimental runs performed to date, 8 vessels were used for dissolution tests (Figure 2.1.2.1a, blue gaskets) with UO_2 based pellets, while 3 vessels were used as blanks to monitor the bulk degradation of H_2O_2 (Figure 2.1.2.1a, red gaskets). For all dissolution experiments pellets with one side polished to mirror finish and the other side only slightly grinded are used.



Figure 2.1.2.1: (a) Experimental setup of the dissolution experiments. (b) Schematic drawing of the experimental vessels for the accelerated dissolution experiments.

The driving force for the UO_2 dissolution in this kind of accelerated dissolution experiment is the oxidative potential of H_2O_2 which is proportional to its concentration in solution. The NaHCO_3 in the solution represents the bicarbonate contained in groundwater. It additionally serves the purpose to prevent the precipitation of U(VI) phases and therefore to ensure a

reliable measurement of the uranium concentration in the solution. Bicarbonate does not intervene directly in the oxidation process, but - with oxidative dissolution - complexes the U(VI) and thus influences the kinetics / driving force, so that the dissolution rate increases with the bicarbonate content [7]. The end of the dissolution process is marked by the accomplishment of a constant uranium concentration in the solution. As stated before this plateau is not due to the limit of U(VI) solubility, but due to the complete consumption of H₂O₂ in the solution.

Due to the previously discovered surface passivation effect when repeatedly employing the same pellets in the dissolution tests, only results from dissolution experiments using pristine pellets were considered for determining the dissolution rates [8]. During the dissolution experiments, solutions were systematically sampled and the H₂O₂ (UV-Vis) and the uranium (ICP-MS) concentrations were determined.

Figure 2.1.2.2 shows the initial dissolution rates of pure UO₂ pellets, normalised to their geometrical surface area, in dependence of their relative density. The (initial) dissolution rates of the pellets were determined from the concentrations of dissolved U(VI) obtained within the first 24 hours of the experiments. A clear dependence of the initial dissolution rates on the density of the pellets is visible with higher initial dissolution rates at lower densities. This is obvious since the initial dissolution rates are normalised to the geometrical surface area and not the real available reactive surface area of the pellets. As lower density means higher porosity, the less dense pellets offer more active surface area for the dissolution of uranium. The following linear dependence of the initial dissolution rate from the theoretical density can be derived:

$$\text{Initial dissolution rate} = 2.02e^{-5} (\pm 2.88e^{-6}) - (1.97e^{-7} (\pm 3.04e^{-8})) * \text{theoretical density}$$

Figure 2.1.2.3 shows the uranium concentration in solution normalised to the geometrical surface area during the first 24 hours of dissolution experiments using pellets with different composition. Symbols of circles represent experiments with pure UO₂, symbols of squares denote experiments with Cr-doped samples and symbols of triangles experiments with a commercially available Cr-doped pellet (AREVA). The results shown in Figure 2.1.2.3 allow to calculate the initial dissolution rates for these experiments. The initial dissolution rates of the pure and the Cr-doped UO₂ pellets are in the range of $1.3 \pm 0.1 \cdot 10^{-6} \text{ mol/m}^2 \cdot \text{s}$ and $0.65 \pm 0.2 \cdot 10^{-6} \text{ mol/m}^2 \cdot \text{s}$, respectively, independent of Cr-doping method, Cr-doping level and grain size. The difference between the dissolution rates of pure UO₂ (for ~ 96 % of theoretical density) and Cr-doped UO₂ pellets (for ~ 98 % of theoretical density) can partly be explained by the slightly lower density of pure UO₂ pellets compared to Cr-doped UO₂ pellets. This finding is underpinned by experiments performed with commercially available Cr-doped UO₂ pellets produced by AREVA exhibiting the same density (~ 96,1 % of theoretical density) as the pure UO₂ pellets produced in the framework of this project. The initial dissolution rates of the AREVA pellets are in the same range as those determined for pure UO₂ pellets.

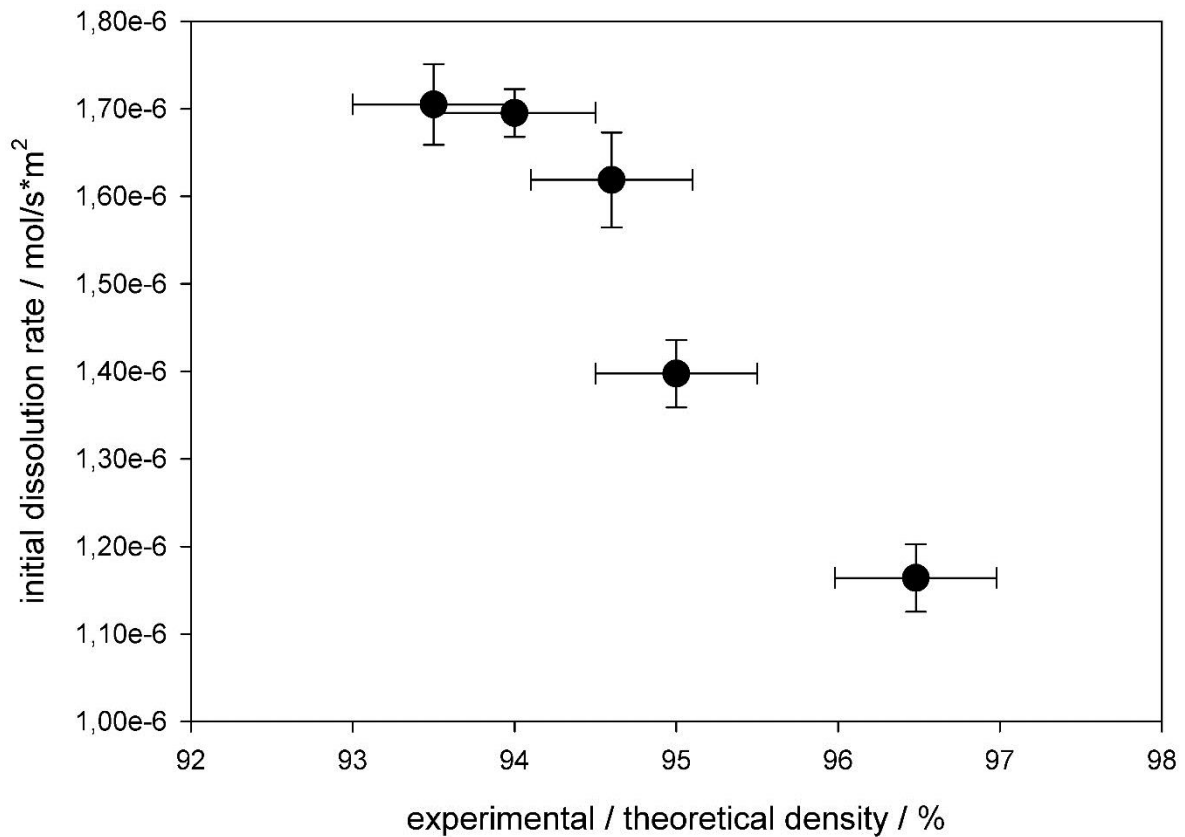


Figure 2.1.2.2: Initial dissolution rates of pure UO_2 pellets, normalised to the geometrical surface area in dependence of relative density ($100 \cdot \text{experimental} / \text{theoretical density}$).

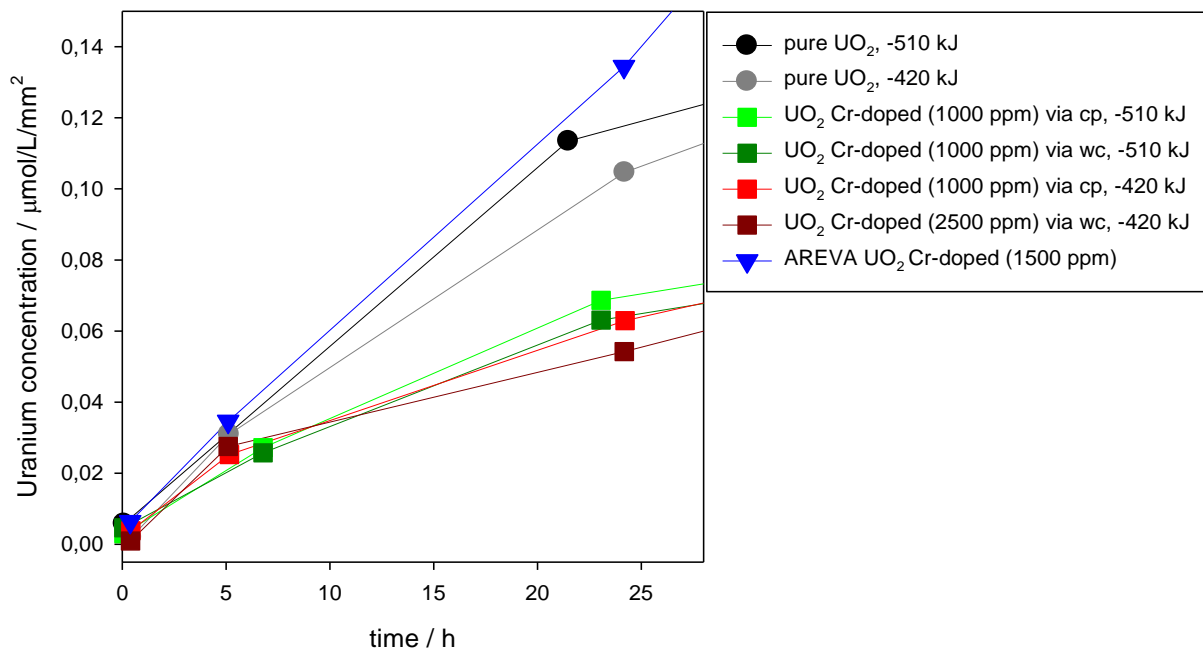


Figure 2.1.2.3: Concentration of uranium in solution normalised to geometrical surface area of pure UO_2 pellets (circles), Cr-doped UO_2 pellets (squares), and commercially available Cr-doped UO_2 pellet (AREVA, triangles). cp = coprecipitation; wc = wet coating; -510 kJ= sinter atmosphere was Ar / 4% H_2 with an oxygen potential ($\Delta G^\circ = -RT \ln P_{O_2}$) of -510 kJ/mol O_2 ; -420 kJ = sinter atmosphere was Ar / 4% H_2 + Ar / 1% O_2 atmosphere with an oxygen potential of -420 kJ/mol O_2 .

Further experiments will be carried out to evaluate the systematic uncertainties of the dissolution experiments (up to now only analytical errors are used). As mentioned in the roadmap of the DisCo project, further dissolution experiments in a young cementitious water (YCWCa) with a pH of ~13.5 will be performed. These dissolution experiments require a redesign of the experimental setup as solutions with high pH would etch the surface of glass, thus PTFE vessels will be tested as reactor vessels. As Ca rich YCW can react with CO₂ from the surrounding air, it has to be tested, if it is necessary to use an additional Ar flushing to prevent the formation of CaCO₃, due to the uptake of CO₂ from air, which would result in a decrease of the solution pH. A transfer of the complete experimental setup into an inert gas glovebox might be an alternative procedure.

2.1.3 Results from VTT

Experimental – The dissolution experiments at VTT are conducted under Ar atmosphere of the glove box. The first experiments were conducted with ²³³U alpha doped UO₂ fragments, already used in dissolution experiments in previous projects [9-14]. These materials are referred as “old” material herein and they are UO₂ materials with 5% or 10% ²³³U alpha doping, simulating the alpha dose of 10000 years old and 3000 years old spent nuclear fuel, respectively. Similar UO₂, without alpha doping (0 %), has been used as a reference. The new pellet materials (UO₂, Cr-doped UO₂, ²³⁸Pu-doped UO₂ and Cr/²³⁸Pu- doped UO₂) will be prepared and characterized by SCK-CEN in collaboration with FZJ. The doping level of ²³⁸Pu-doped UO₂ pellets, to be fabricated, will correspond to the alpha dose of ~10 000 years old nuclear fuel. Fabrication of these materials has been delayed from 2019. The delivery to Finland was arranged in the beginning of June 2020 as the final batch of Pu-doped pellets was ready.

The leaching experiments are conducted mainly in natural groundwaters. Some parallel experiments will be conducted also in bicarbonate water with “new” Cr- doped materials. Natural groundwaters have been sampled from the Olkiluoto site, which is the planned site for disposal of spent nuclear fuel in Finland.

Natural groundwaters

In the previous EU project, REDUPP [13, 14], 3 different groundwaters from different depths (fresh, brackish, saline) were used in leaching experiments of UO₂. In the DisCo project the experiments with ²³³U-doped UO₂ are conducted in brackish OL-KR6 (cf. Table 2.1.3.1), because previous experiments have shown slight solubility increasing effect with 10% alpha doping under same groundwater conditions [13, 14]. Brackish, high carbonate water does not represent the current groundwater conditions at the disposal level (app. - 400 m). However, this kind of conditions might occur for example in the postglacial situation, if the groundwater layers will be strongly mixed at the Olkiluoto site.

Table 2.1.3.1: Composition of natural groundwaters OL-KR6 (brackish) and ONK-KR15 (saline) to be used in DisCo dissolution experiments. Two columns for OL-KR6 show the slight temporal variation and ONK-KR15 are given as average values from data collected from 2011 to 2018.

	OL-KR6 (2013)	OL-KR6 (2016)	ONK-KR15 (2011-2018)
pH	7.6	7.6	8.0
Ammonium, NH ₄ (mg/l)	0.31	0.29	0.025
Bicarbonate, HCO ₃ (mg/l)	159	153	9.7
Bromide, Br (mg/l)	12	11	46
Calcium, Ca (mg/l)	540	530	1242
Chloride, Cl (mg/l)	3340	3340	6162
Dissolved inorg carbon (mg/l)	27	31	1.8
Fluoride, F (mg/l)		0.4	1.6
Iron, Fe (total) (mg/l)	0.36	0.28	0.01
Iron, Fe ²⁺ (mg/l)		0.28	0.015
Magnesium, Mg (mg/l)	151	151	33
Nitrate, NO ₃ (mg/l)	0.4	0.4	<0.04
Nitrite, NO ₂ (mg/l)	0.2	0.2	<0.02
Nitrogen, N(Total) (mg/l)	0.36		0.077
Non Purgeable Organic Carbon (mg/l)	4.6	5.1	3.5
Phosphate, PO ₄ (mg/l)		0.2	0.2
Potassium, K (mg/l)	18	18	10
Silicate, SiO ₂ (mg/l)	11	12	6.3
Sodium, Na (mg/l)	1460	1460	2392
Strontium, Sr (mg/l)	5.5	5.8	10.2
Sulphate, SO ₄ (mg/l)	404	406	0.33
Sulphide, S ₂ ⁻ (mg/l)		0.02	0.05
Sulphur, S (total) (mg/l)	130	130	0.6
Total dissolved solids (mg/l)	6101	6088	9913
Carbonate alkalinity, HCl uptake (mmol/l)	0.05	0.05	<0.05
Total acidity, NaOH uptake (mmol/l)	0.18	0.16	0.05
Total alkalinity, HCl uptake (mmol/l)	2.6	2.5	0.16

ONK-KR15 groundwater has been selected for the leaching experiments of new UO₂ materials fabricated in the DisCo project. ONK-KR15 stands for the ONKALO characterization drill core at the depth of -399 m. This groundwater represents groundwater conditions at the disposal level. It has less sulphate and carbonate (0.16 mM) in comparison to OL-KR6 (2.5 mM HCO₃⁻), but relatively low salinity compared to saline waters (see Table 2.1.3.1). ONK-KR15 water resembles the composition of saline OL-KR5 used previously in REDUPP experiments, but ONK-KR15 was selected instead due to unavailability of OL-KR5. It represents groundwater water, which has not been mixed with other water types. These kind of low carbonate and saline groundwater conditions prevail at disposal sites (-500 to -400 m bgl) in Finland and Sweden, and are also possible in future scenarios. Thus, it is relevant to gain information the possible effect of low carbonate concentrations in comparison to bicarbonate (1 to 2 mM) concentrations used in many reference waters in DisCo project.

OL-KR6 ground water was sampled at the continuous measurement station on the ground in June 2018. The alkalinity and pH of the groundwater were periodically measured under glove box conditions. Both pH and alkalinity showed slight increase during 300 days equilibration period in the glove box (see Figure 2.1.3.1). This may be the effect of degassing of CO₂ under Ar atmosphere. The elemental concentrations and pH of OL-KR6 are followed during the experiments to evaluate the representativeness of OL-KR6 water.

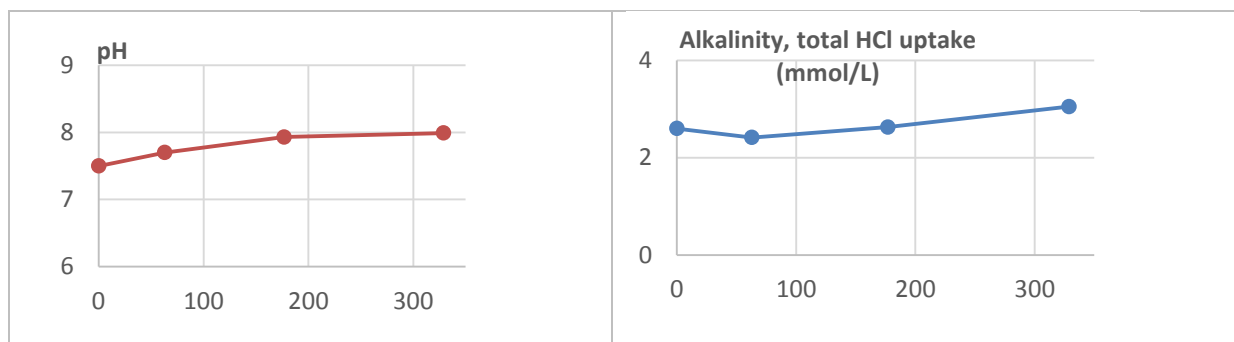


Figure 2.1.3.1: Evolution of pH and alkalinity of OL-KR6 ground water during 300 days period under glove box conditions.

One litre of the KR-6 groundwater was allowed to equilibrate with iron strips to sweep the natural uranium away from the groundwater before starting the actual dissolution experiments. The initial uranium concentration decreased from $5 \cdot 10^{-9}$ mol/L to $1 \cdot 10^{-11}$ mol/L. Due to formation of black precipitates, the water was also filtered with syringe and $0.22 \mu\text{m}$ filter prior to leaching experiments. ONK-KR15 was sampled from underground research facility ONKALO, in Olkiluoto in early April 2020. Some experiments will be also conducted with Cr doped material in bicarbonate FIN water (19 mM NaCl and 1 mM NaHCO_3), as a reference and to allow for comparability of results of other working groups within the DisCo project.

Leaching experiments

The old samples, ^{233}U alpha doped UO_2 fragments (see Table 2.1.3.2), had been stored under anaerobic glove box conditions for 4 years. There are parallel samples (2-0 and 1-0, 1-5 and 2-5, 1-10 and 2-10) for 1 g samples and only one sample per doping level with higher mass (~ 3 g). The previous dissolution experiments had been carried under saline groundwater and thus, the samples required preparation before experiments by pre-leaching twice with bicarbonate solution before start of the actual experiments in natural groundwater. This removed salts possibly precipitated during the storage period.

Table 2.1.3.2: Composition of 0 %, 5% and 10 % ^{233}U doped pellets including the sample masses.

UO_2 phase	^{233}U (%)	^{235}U (%)	^{238}U (%)	$^{235}\text{U}/^{238}\text{U}$	Samples (g)
Un-doped	0	2.82	97.18	0.029	1, 1, 3 g
5% ^{233}U -doped 15.7 MBq/g	5.0	4.5	90.5	0.050	1, 1, 3 g
10% ^{233}U -doped 31.4 MBq/g	10.0	4.5	85.5	0.053	1, 1, 2.5 g

The experimental system for dissolution tests is described in Figure 2.1.3.2, showing the test vessel with an iron strip leaning to vessel wall, and UO₂ fragments placed into a glass saucer, which functions as a holder for the UO₂ fragments. The iron foil maintains the reducing conditions, producing some H₂. It also mimics the cast iron insert of the copper canister that will be present next to spent nuclear fuel in the repository.

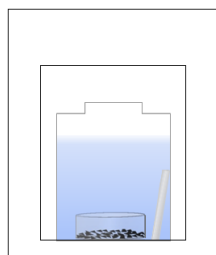


Figure 2.1.3.2: Schematic view of closed plastic vessel (V=60 ml) (left) in which the experiments will be conducted in the anaerobic glove box (right). UO₂ fragments are placed in the glass saucer and the iron strip is leaning on the vessel wall in leaching media.

The experiments were set-up by adding 40 ml of filtered OL-KR6 groundwater and one piece of iron foil (1.5 cm x 3 cm) into 60 ml polypropylene vessel and this was allowed to equilibrate for 2 days before addition of UO₂ solids. The iron foils were cut and gently polished from Goodfellow iron foils (100 mm x 100 mm x 0.125 mm, 99.5 % Fe). After pre-washing in bicarbonate solution, UO₂ fragments were rinsed twice with 2 ml of MQ-water, and allowed to dry for a short moment, before weighting them into a clean saucer. The saucer with fragments was placed on the bottom of the test vessel. Prior to the spike of ²³⁵U-rich solution, 168 µl of 0.01 M NaOH was added to neutralize the acid content of the spike. Next, the solution spike ²³⁵U/²³⁸U ~10/1 was added to give an initial total U concentration of 3.4·10⁻⁹ mol/L and the solution was stirred with the tip of the pipette before closure.

The first samples (t=0) were taken already made before the addition of UO₂ fragments. The following samples, 1.2 ml, were taken in the time intervals 2 h, 1, 4, 12, 41, 61, 105, and 201 days. The sample volume was compensated with addition of filtered OLK-KR6 groundwater. The samples were acidified with 12 µl of suprapure HNO₃ (ULTREX II by J.T. Baker). Uranium concentration and isotope ratio ²³⁵U/²³⁸U was measured with sector field ICP-MS (Element 2 by ThermoScientific). The analyses have been run from 1/5 diluted samples with APEX IR sample introduction system, which intensifies the signal of uranium approximately 7 fold in comparison with standard spray chamber with Peltier cooling.

Results and discussion – Figure 2.1.3.3 shows the evolution of the measured ²³⁸U concentrations in the DisCo leaching experiments with ~1 g and ~3 g samples in OL-KR6 water with different doping levels (0, 5 or 10 % indicated in the second number of the test code). In all experiments, the concentration of ²³⁸U has settled at the level between 2·10⁻¹¹ and 5·10⁻¹¹ mol/L after 200 days. The 1 g sample with doping level 5% (1-5) shows slightly lower concentration levels compared to the other 1 g samples.

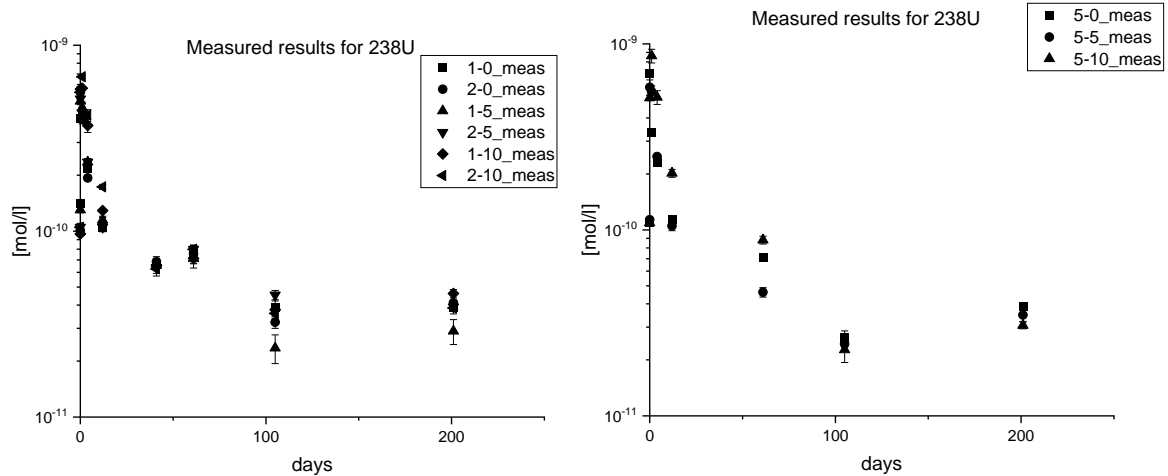


Figure 2.1.3.3: Evolution of ^{238}U concentrations in the DisCo leaching experiments with ~ 1 g (2-0 and 1-0, 1-5 and 2-5, 1-10 and 2-10) and 3 g (5-0, 5-5-, 5-10) samples in OL-KR6 water with different doping levels (0, 5, or 10%) during 200 days of experiment.

In comparison to parallel experiments conducted in REDUPP project [13, 14], the concentration of ^{238}U has settled at slightly higher level with 1 g samples than in REDUPP experiments, even though the magnitude of the difference is small. In the case of 3 g samples, with higher surface to volume ratio, the concentration of ^{238}U has settled at lower or same level than in REDUPP experiments. In these experiments, different doping levels did not show notable difference in the concentration levels.

In addition to concentrations, the isotopic ratio $^{235}\text{U}/^{238}\text{U}$ was measured in the liquid samples. The initial ratio of 7.9 drops below 1 in after 10 days and below 0.1 after 50 days in all experiments and decreases further during the 200 days experiment. When taking into account the original ratios in solid and aqueous phase and the change and the original concentration, the ratio can be used to calculate the cumulative release from solid phase to solution.

Figure 2.1.3.4 shows the comparison of the measured ^{238}U concentrations (solid) in comparison to the ones calculated from original concentrations and the change in isotopic ratio during the experiment. The isotopic method reveals that the cumulative uranium release during the 200 days experiment can be at the magnitude of 10^{-7} mol/L. The calculations tend to produce bigger errors (see Figure 2.1.3.4) as the experimental time extends, because more iteration rounds are used to calculate the concentrations from initial values at the final sampling point.

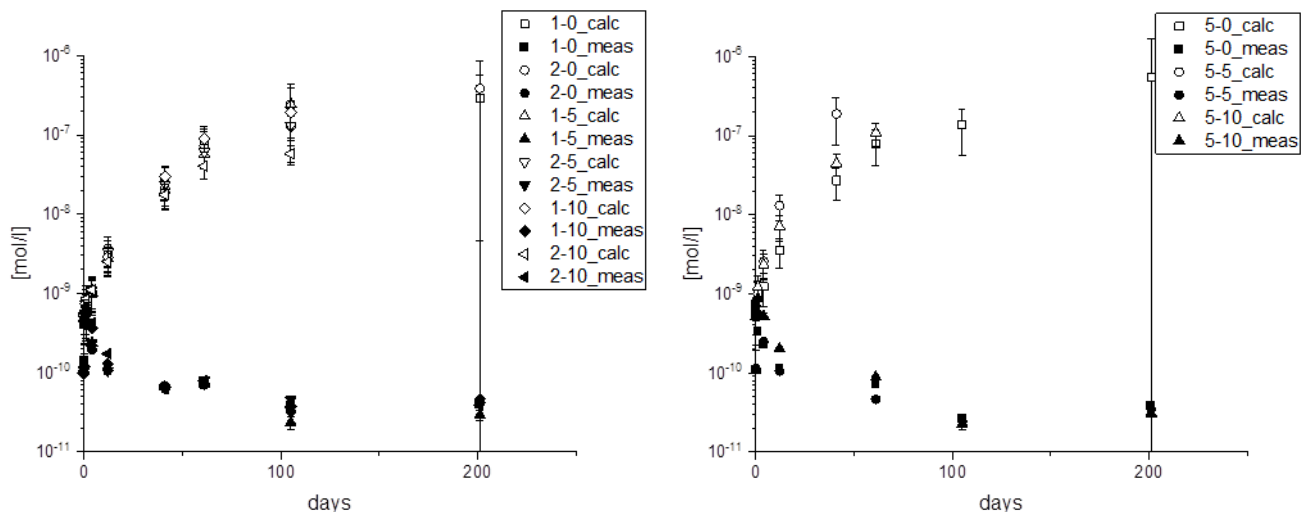


Figure 2.1.3.4: Evolution of the measured ^{238}U concentrations (solid) in DisCo leaching experiments with 1 g (left) and ~3 g (right) in OL-KR6 water in comparison to cumulative release (hollow symbols) calculated with isotopic dilution method.

Conclusions – During the 200 days experiments the solubility of uranium settles between $2 \cdot 10^{-11}$ and $5 \cdot 10^{-11}$ mol/L. However, the cumulative release, calculated from isotopic dilution, indicates total release during 200 days has increased above $1 \cdot 10^{-7}$ mol/L. This describes the amount of total release when dissolution and precipitation/sorption are taking place simultaneously. There is no remarkable difference in the measured concentrations between different doping levels. Calculated cumulative concentrations show more scattering, but probably more detailed data analysis is needed to conclude any effects of doping levels as the uncertainties seem to be also larger for calculated concentrations. Thus, clear indication of the effect of doping level could not be observed in OL-KR6 groundwater. The next experimental series with UO_2 , $\text{UO}_2 + ^{238}\text{Pu}$ -doping, $\text{UO}_2 + \text{Cr}$ and $\text{UO}_2 + \text{Cr} + ^{238}\text{Pu}$ will give information, if the Cr-doping will show any effects on the solubility of UO_2

2.1.4 Results from CIEMAT

To understand the matrix dissolution of modern LWR fuels and in particular the effect of Cr on the dissolution rate of the spent fuel, Cr, Cr/Al and Gd-doped materials have been prepared within WP2 of this project. These model materials have been exposed to three reference waters (inert system NaClO_4 at pH 7.2, bicarbonate water at pH 8.9 and young cementitious water at pH 13.5) relevant for geological disposal in 4.7% H_2/N_2 atmosphere, initially assumed as reducing conditions but unforeseen oxygen intrusion must have occurred due to the unexpectedly high U concentrations found. The role of perchlorate system used as a blank test (without carbonate) is to adjust low ionic strength with a non-complexing agent because of its low reactivity in order to be compared with BC and YCW-Ca systems. The model materials synthesised according to a protocol developed within the WP2 of this project at CIEMAT along the first year of the project, have been used to start the leaching tests in the second trimester of 2018, while the improved fabrication procedure of Cr doped UO_2 will be completed in the second trimester of 2020.

A first batch of doped UO_2 disks was leached and once the fabrication of new improved Cr- UO_2 samples will be completed, new leaching tests are foreseen in the first semester 2020. In anticipation of the improved model materials, preparatory leaching experiments were performed at 4.7% H_2/N_2 . Static dissolution experiments were started in the first semester of 2018 with doped UO_2 , either in inert water (PC: NaClO_4 20 mM) at pH 7.2, bicarbonate solution (BC: 19mM NaHCO_3 + 1 mM NaCl) at pH 8.5 and Young Cementitious Water at pH 13.5 (YCW-6). Further details about the simulated water compositions are shown in Table 2.1.4.1 (YCW-Ca light was improved with regard to the last meeting by bettering reagents purity and lowering Ca content, see column YCW-3 at Table 2.1.4.1). All tests were performed in an Ar glove box at room temperature in autoclaves under 7-8 bar 4.7% H_2/N_2 (inert system without Pt and BC and YCW-Ca with a Pt wire, in which sample disk was suspended). Even though in previous description of experiments, in the 1st and 2nd annual meetings, O_2 concentration in the glove box was reported to be below 2 ppm, a failure of oxygen sensor was identified during the latest experiments (YCW) and hence, real concentration reached was 1000 ppm along all the tests. Stainless steel autoclaves with a PEEK insert were described in previous report [5]. For this dissolution experiments, the pellets were first annealed at 1000 °C in reducing conditions. Aliquots of aqueous phase were collected through a sampling valve without opening the reactor, due to the overpressure inside the reactor. Then, autoclaves were refilled with 4.7% H_2/N_2 up to 8 bar.

Filtered (GHP Acrodisc, PALL, 0.2 μm) and ultrafiltered (Amicon Ultra-4 3k de Millipore, < 2 nm) samples were measured by ICP-MS to quantify dissolved U concentrations. However, for a better measurement of U in solution this filtration procedure was changed from the sixth sampling in YCW-Ca experiments, therefore samples were not-filtered and ultrafiltered. At the end of each experiment, autoclaves were rinsed with 2 M HNO_3 in order to estimate the amount of U sorbed on the system. A summary of dissolution tests performed up to now is shown in 2.1.4.2.

Table 2.1.4.1: Composition of the synthetic aqueous media.

Conc / molc ⁻¹	PC-1	BC-1	YCW-3	YCW-6
Na	2.18·10 ⁻²	2.1·10 ⁻²	1.35·10 ⁻¹	1.3·10 ⁻¹
Mg	2.07·10 ⁻⁶	1.48·10 ⁻⁶	2·10 ⁻⁶	<LOQ
Al	3.61·10 ⁻¹⁰	3.55·10 ⁻⁹	5.0·10 ⁻⁸	4·10 ⁻⁹
K	2.80·10 ⁻⁴	1.40·10 ⁻⁴	3.46·10 ⁻¹	3·10 ⁻¹
Ca	2.89·10 ⁻⁶	5.6·10 ⁻⁶	7.8·10 ⁻⁴	1.7·10 ⁻⁴
Cr	1.9·10 ⁻⁹	4·10 ⁻⁹	7·10 ⁻⁸	9.2·10 ⁻⁸
Mn	7.0·10 ⁻⁹	1.9·10 ⁻⁸	1.6·10 ⁻⁷	3·10 ⁻⁸
Fe	3.4·10 ⁻⁸	9·10 ⁻⁸	9.3·10 ⁻⁷	4.2·10 ⁻⁷
Co	3.9·10 ⁻¹⁰	1.43·10 ⁻⁹	1.8·10 ⁻⁹	<LOQ
Ni	<1.7·10 ⁻⁹	<1.7·10 ⁻⁹	<1.7·10 ⁻⁹	<LOQ
Cu	2.3·10 ⁻⁹	1.2·10 ⁻⁸	2.2·10 ⁻⁷	9.7·10 ⁻⁸
Cs	1.9·10 ⁻¹⁰	1.38·10 ⁻⁹	1.7·10 ⁻⁹	2.3·10 ⁻¹⁰
Ba	9.9·10 ⁻⁹	1.8·10 ⁻⁸	1.4·10 ⁻⁷	1.9·10 ⁻⁸
Ce	7.1·10 ⁻¹²	1·10 ⁻¹⁰	<7·10 ⁻¹²	<LOQ
Gd	9·10 ⁻¹²	8·10 ⁻¹¹	<6·10 ⁻¹²	<LOQ
Pb	5.7·10 ⁻¹⁰	5.3·10 ⁻⁹	4.0·10 ⁻⁸	1.5·10 ⁻⁸
Th	<4.3·10 ⁻¹²	<4.3·10 ⁻¹²	<4.3·10 ⁻¹²	<LOQ
U	1.2·10 ⁻¹⁰	3.6·10 ⁻⁹	5.9·10 ⁻⁹	<LOQ
Cl ⁻	1.0·10 ⁻⁴	1.1·10 ⁻³	3.9·10 ⁻⁴	1.5·10 ⁻⁸
SO ₄ ²⁻	-	3.3·10 ⁻⁵	2.5·10 ⁻⁴	1.9·10 ⁻³
pH	7.2±0.1	8.9±0.1	13.5±0.1	13.5±0.1

Table 2.1.4.2: Summary of samples and leaching conditions of autoclaves with 4.7% H₂/N₂.

Experiment ID #	Solid material	wt% dopant	BET and geometrical surface area	Grain diameter (mm)	type of Solution System
1-UO₂-Cr-B (412)	Cr-doped UO ₂	0.06%	0.63±0.02(0.0001985)	10.16±1.17	NaClO ₄
2- UO₂-Gd-B (440)	Gd-doped UO ₂	4.5%	0.63±0.01 (0.0002057)	0.5±0.08	NaClO ₄
3- UO₂-Cr/Al-B (401)	Al-Cr-doped UO ₂	0.05%/0.02%	0.25±0.01 (0.0002094)	9.87±1.02	NaClO ₄
4- UO₂-Cr-BC (450)	Cr-doped UO ₂	0.06%	0.63±0.02(0.0001985)	10.16±1.17	Bicarbonate water
5- UO₂-Gd-BC (457)	Gd-doped UO ₂	4.5%	0.63±0.01 (0.0002057)	0.5±0.08	Bicarbonate water
6- UO₂-Cr/Al-BC (405)	Al-Cr-doped UO ₂	0.05%/0.02%	0.25±0.01 (0.0002094)	9.87±1.02	Bicarbonate water
7- UO₂-Cr-YCW (451)	Cr-doped UO ₂	0.06%	0.63±0.02(0.0001985)	10.16±1.17	YCWCa
8- UO₂-Gd-YCW (441)	Gd-doped UO ₂	4.5%	0.63±0.01 (0.0002057)	0.5±0.08	YCWCa
9- UO₂-Cr/Al-YCW (400)	Al-Cr-doped UO ₂	0.05%/0.02%	0.25±0.01 (0.0002094)	9.87±1.02	YCWCa

Figure 2.1.4.1 a), b) and c) illustrate the U released vs time for dissolution of a) UO_2 -0.06wt% Cr_2O_3 , b) UO_2 -0.05wt% Cr_2O_3 -0.02wt% Al_2O_3 and c) UO_2 -4.5wt% Gd_2O_3 . Based on the first series of tests, the H_2 atmosphere ($p_{\text{H}_2} = 0.37 \pm 1\text{bar}$) was not capable to maintain system reducing conditions, as it is suggested from data. Filled symbols correspond to filtered (or not-filtered) and empty symbols to ultrafiltered samples quantified by ICP-MS. The U concentration in the solutions reached plateau levels in PC and YCW-6, but not in BC.

At $\text{pH} = 7.2$ (PC) the filtered U concentration remains close to 10^{-9} M for the three doped UO_2 samples over the whole test duration (~ 140 d), close to the solubility limit of 10^{-8} - 10^{-9} M [15]. At $\text{pH} 8.9$ (BC), higher U concentrations are quantified compared to those at 7.2 ($\sim 10^{-6}$ M for Cr-doped UO_2 , $\sim 10^{-7}$ M for Cr/Al-doped UO_2 and $\sim 10^{-8}$ M for Gd-doped UO_2). The trend of U concentration in solution shows that there is a slight increase in dissolution with time for the Cr-doped UO_2 in BC with no plateau when compared with PC or YCW-6 media. This could be caused by oxidation/dissolution of the pellet surface, promoted by the complexing agent HCO_3^- . Nevertheless, as it was suggested by USFD in [15] more analysis for longer time periods is required. At $\text{pH} = 13.5$, U concentrations are similar to those in the tests in BC, despite the highest $\text{HCO}_3^-/\text{CO}_3^{2-}$ concentration measured in YCW-6 (0.45 M) and for both, no differences were found between filtered/not-filtered and ultrafiltered samples. Ollila [16] pointed out the redox sensitivity of the U solubility at strongly alkaline pH like cement pore water conditions. It suggests that the measured Eh (YCW-6) in these experiments in the range of -9 to -40 mV could be enough to increase the U concentrations even if in BC the Eh has been found to be higher (70 – 138 mV).

We can confirm with the current data that U is extremely sensitive to oxidative dissolution at high pH (13.5). The almost negligible differences between filtered/not-filtered and ultrafiltered samples are considered as an indication that there was no colloids formation for any of the experiments.

The normalised dissolution rates of U ($R_L(\text{U})$ in $\text{g}\cdot(\text{m}^2\text{d})^{-1}$) as a function of time were calculated from the concentrations of dissolved U, the geometric surface area, the U mass fraction in the solid sample and the initial mass of sample. Generally, the normalized dissolution rate profile decreased vs time, as shown in Figure 2.1.4.2 for samples a) UO_2 -0.06wt% Cr_2O_3 , b) UO_2 -0.05wt% Cr_2O_3 -0.02wt% Al_2O_3 and c) UO_2 -4.5wt% Gd_2O_3 .

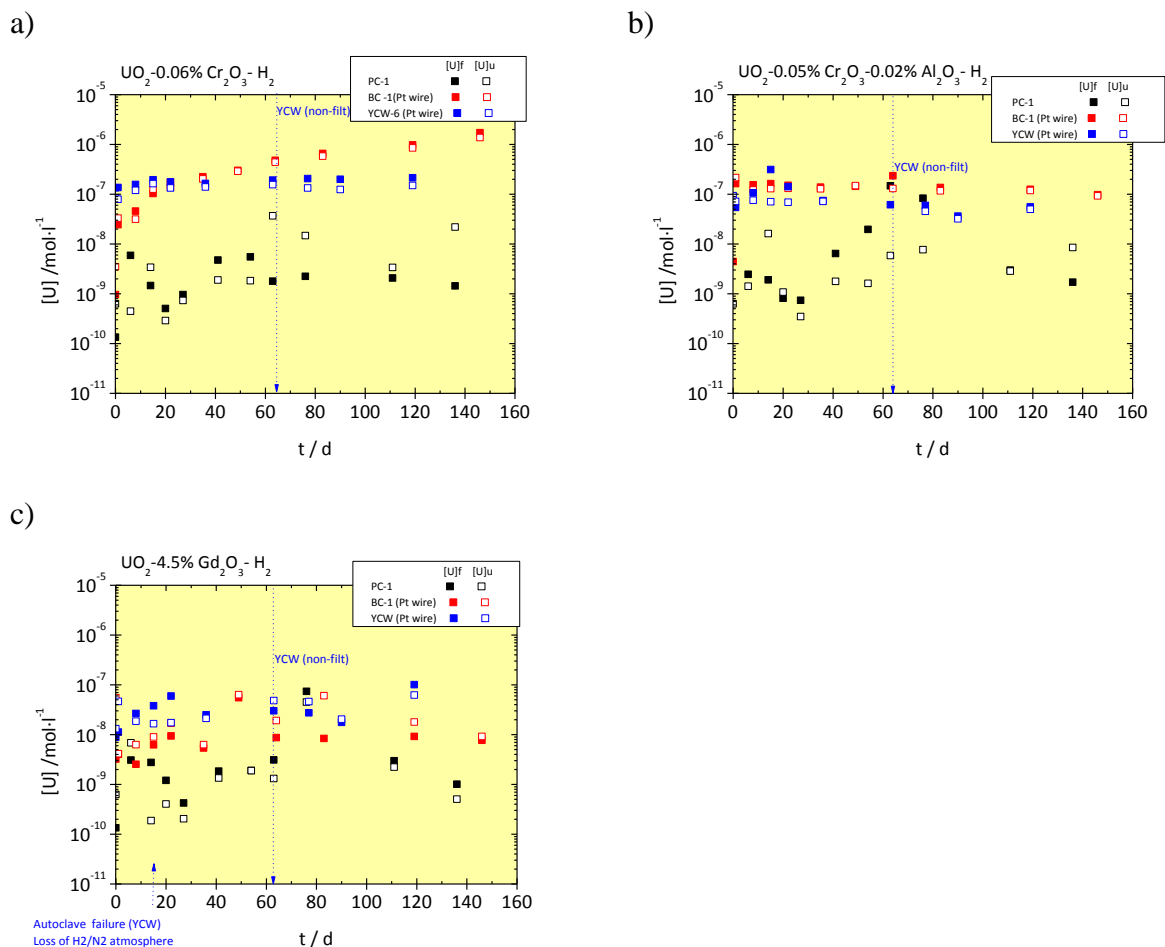


Figure 2.1.4.1.: U concentration measured for the first test series of a) $\text{UO}_2-0.06\text{wt}\% \text{Cr}_2\text{O}_3$, b) $\text{UO}_2-0.05\text{wt}\% \text{Cr}_2\text{O}_3-0.02\text{wt}\% \text{Al}_2\text{O}_3$ and c) $\text{UO}_2-4.5\text{wt}\% \text{Gd}_2\text{O}_3$ in 0.02M NaClO_4 ($\text{pH} = 7.2$), 0.019M NaHCO_3 ($\text{pH} = 8.9$, Pt wire) and YCW-6 ($\text{pH} = 13.5$, Pt wire) in autoclave experiments ($\text{pH}_2 = 0.37 \pm 1$ bar) at 22 ± 3 °C. Filled symbols represent filtered (or not-filtered) and empty symbols are ultrafiltered.

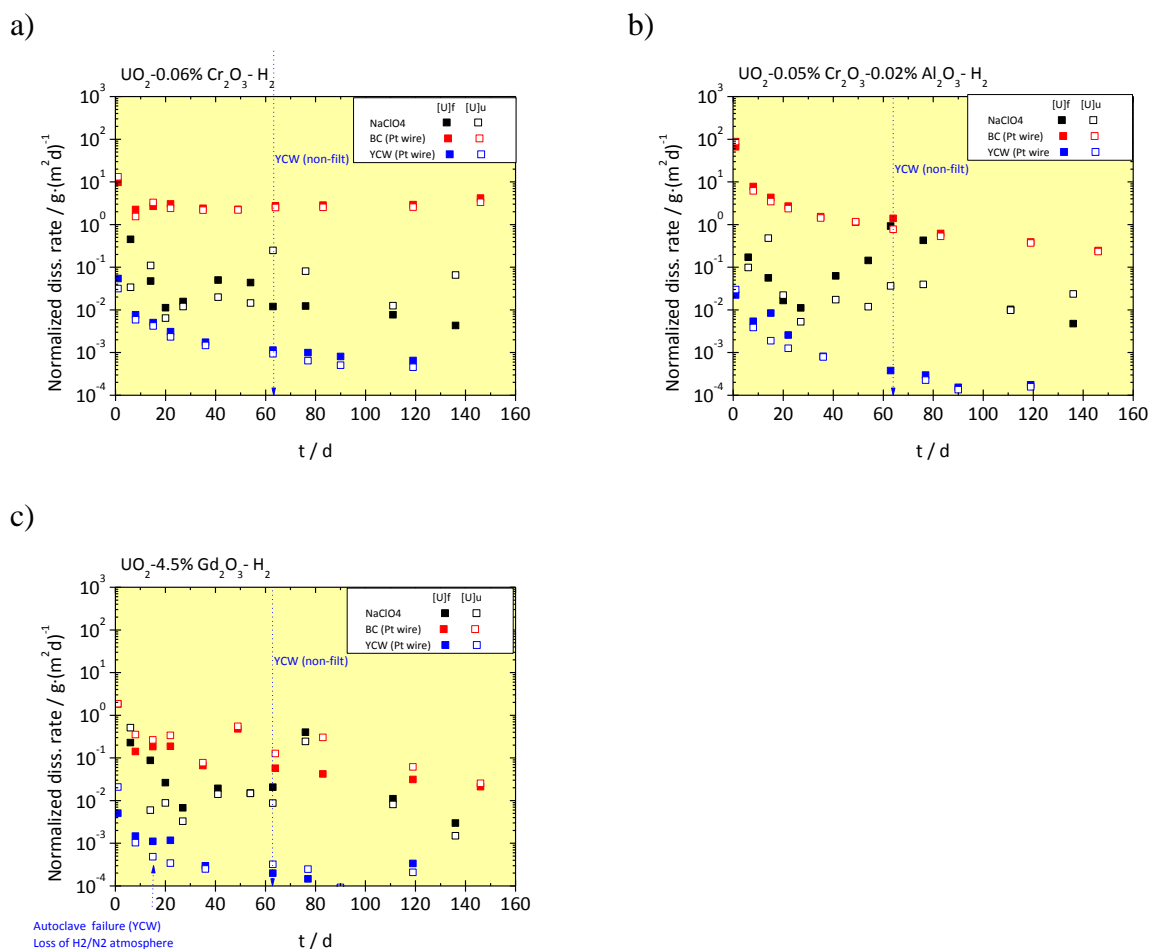


Figure 2.1.4.2: $R_L(U)$ for the first test series of a) UO_2 -0.06wt% Cr_2O_3 , b) UO_2 -0.05wt% Cr_2O_3 -0.02wt% Al_2O_3 and c) UO_2 -4.5wt% Gd_2O_3 in 0.02M $NaClO_4$ ($pH = 7.2$), 0.019 M $NaHCO_3$ ($pH = 8.9$, Pt wire) and YCW-6 ($pH = 13.5$, Pt wire) in autoclave experiments ($pH_2 = 0.37 \pm 1$ bar) at 22 ± 3 °C. Filled symbols represent filtered (or not-filtered) and empty symbols are ultrafiltered.

For the sake of simplicity, even though $R_L(U)$ values have been plotted in $g \cdot (m^2 d)^{-1}$ as other colleagues in the project, all of them have been re-calculated in $mol \cdot (m^2 d)^{-1}$ for comparison to literature data.

In PC solution ($pH = 7.2$), the initial/final dissolution rates were found to be $2 \cdot 10^{-3}$ to $3 \cdot 10^{-5}$ $mol \cdot (m^2 d)^{-1}$ for the Cr-doped UO_2 pellet, $7 \cdot 10^{-4}$ to $3 \cdot 10^{-5}$ $mol \cdot (m^2 d)^{-1}$ for the Cr/Al-doped UO_2 and $1 \cdot 10^{-3}$ to $3 \cdot 10^{-5}$ $mol \cdot (m^2 d)^{-1}$ for the Gd-doped UO_2 . Taking into account the low geometric surface area, the final U dissolution rates for the shown pellets are quite similar, it seems that the dopant has no significant effect on the dissolution rates of these UO_2 -based materials, although Gd- UO_2 that has been found to have the lowest value.

In BC solution ($pH = 8.9$), normalised dissolution rates were significantly higher, as the bicarbonate concentration was higher than other values used in literature. In this media the initial/final dissolution rates were found to be $4 \cdot 10^{-2}$ to $2 \cdot 10^{-2}$ $mol \cdot (m^2 d)^{-1}$ for Cr-doped UO_2 pellet, $3 \cdot 10^{-1}$ to $1 \cdot 10^{-3}$ $mol \cdot (m^2 d)^{-1}$ for the Cr/Al-doped UO_2 and $8 \cdot 10^{-3}$ to $9 \cdot 10^{-5}$ $mol \cdot (m^2 d)^{-1}$ for the Gd-doped UO_2 . The obtained data are far from those obtained by Gimenez et al. [17]

for unirradiated UO_2 in flow through reactors using $[\text{HCO}_3^-]$ at 10^{-3} M. The aforementioned authors of the flow through experiments reported a dissolution rate of U of $9 \cdot 10^{-6} \text{ mol} \cdot (\text{m}^2\text{d})^{-1}$.

In YCW-6 solution (pH = 13.5), the normalised dissolution rates were significantly higher as the bicarbonate concentration was higher than other values used in literature. In this medium the initial/final dissolution rates were found to be $2 \cdot 10^{-4}$ to $3 \cdot 10^{-6} \text{ mol} \cdot (\text{m}^2\text{d})^{-1}$ for Cr-doped UO_2 pellet, $9 \cdot 10^{-5}$ to $7 \cdot 10^{-7} \text{ mol} \cdot (\text{m}^2\text{d})^{-1}$ for the Cr/Al-doped UO_2 and $2 \cdot 10^{-5}$ to $9 \cdot 10^{-7} \text{ mol} \cdot (\text{m}^2\text{d})^{-1}$ for the Gd-doped UO_2 .

SEM, XRD and Raman measurements on pellets after the dissolution experiments are in progress and will complement the picture of data obtained. In addition, more studies of the dissolution as a function of dopant concentration are essential to predict this effect at long-term behaviour.

2.2 MOX related model systems

2.2.1 Results from CEA

Experimental – The leaching experiment took place in two stages: a first stage of corrosion of the iron foil in a synthetic CO_x groundwater (84 days) followed by a leaching experiment of two MOX pellets in the study environment (468 days). This part presents all the results obtained in terms of solution analyses, mass balances and characterization of the leached surfaces. A proposal of mechanisms is also put forward to explain these experimental results which are also the subject of a modelling task in WP5 of the DisCo project.

Iron foils were placed in the autoclave to simulate container corrosion products and to move towards realistic reducing conditions in the absence of the fuel pellet. Such reducing conditions are expected in deep geological disposal. Rolled 99.99% pure iron foils were purchased from Goodfellow. Their size was 2.5 cm by 2.5 cm for a thickness of 125 μm and a weight of around 0.64 g. One iron foil was used for the leaching experiment. Before being set up in the reactor, the foil was rinsed in ethanol and ultrasound-cleaned for 2 minutes.

The iron foil was first pre-corroded in 180 mL of synthetic CO_x water for around 80-90 days in the absence of the MOX pellets. This first step was intended to ensure the presence of corrosion products on the iron foil surface, to obtain a solution chemistry containing Fe^{2+} ions not initially present in the synthetic CO_x water, and to have reducing conditions when the MOX pellets were introduced at a later date. The iron foil was slightly curved to enable maximum contact with water, and placed on the platform immediately under the pellet support. Once the leaching reactor had been closed, it was purged with a mixture Ar/CO_2 3000 ppm for 2h30 and then put under a pressure of 3.5 bars. The leaching solution was regularly sampled over 84 days.

After the iron pre-corrosion phase, the reactor was opened to add two homogeneous MOX pellets ($\text{U}_{0.73}\text{Pu}_{0.27}\text{O}_2$) with an alpha activity of $2.2 \cdot 10^9$ Bq/g, which were placed on a support above the iron foil. The reactor was then closed again, purged with a mixture of Ar/CO_2 3000

ppm for 30 min, and returned to a pressure of 3.5 bars with the same gas mixture. Samples of the leaching solution were regularly collected over time.

Results – The concentrations of COx water elements were monitored (Ca, K, Mg, Na, Si, Sr, Fe). Most of the element concentrations were found to be constant over the duration of the experiment (including the pre-corrosion phase), except for calcium, strontium, silicon and iron. The evolution of the concentrations of these elements is shown in Figure 2.2.1.1. The calcium and strontium concentrations are decreasing over time (from 330 to 280 mg L⁻¹ for calcium and from 20 to 14 mg L⁻¹ for strontium), probably indicating the precipitation of secondary phases, which will be looked for during the solid analyses.

The iron concentration increases during the pre-corrosion stage until reaching a plateau around 20 mg L⁻¹, suggesting a thermodynamic equilibrium with a secondary phase (corrosion product). After adding fuel pellets, the increase in iron concentration resumes and seems to reach a second level of around 70 mg L⁻¹. Over the long term, the concentration of iron in solution gradually decreases. It is possible that these levels and the final decrease are due to the precipitation / dissolution of different iron-based phases, which will be sought during the characterizations of the solid. Anoxic corrosion of metallic iron is clearly the main source of iron into the solution as demonstrated by the presence of H₂ in the gas phase with a content of 13,800 ppm after 468 days of leaching.

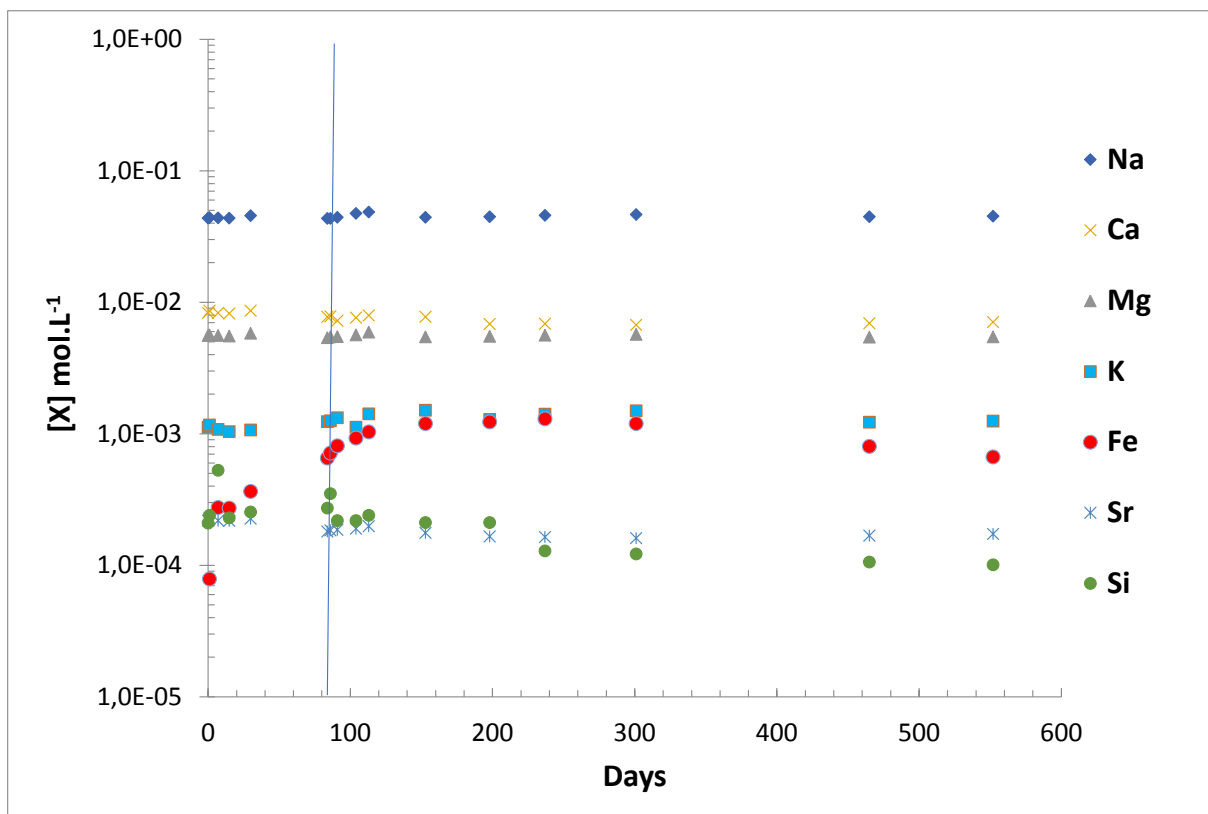


Figure 2.2.1.1: Evolution of the chemistry of synthetic COx groundwater over time (84+468 = 552 days). The vertical bar corresponds to the end of the pre-corrosion stage (84 days) and to the introduction of the MOX pellets into the reactor.

The samplings also allowed monitoring over time of the actinides concentrations and the physico-chemical parameters (Eh and pH). The pH was constant during the experiment, at a value of 8.2 ± 0.2 . The redox potential was measured around -0.1 ± 0.03 V / SHE directly in the leachate after opening the reactor at the end of the experiment. The measurements in the intermediate samples were more unstable. The concentrations of H_2O_2 and Pu were below the detection limits of the methods used that is 10^{-7} mol L⁻¹ for H_2O_2 and 5×10^{-10} mol L⁻¹ for Pu.

Concerning the uranium concentrations, the results indicate a significant effect of iron on the oxidative dissolution of this homogeneous MOX fuel. Uranium concentrations are less than $1 \mu\text{g L}^{-1}$ after few months of leaching (Figure 2.2.1.2). Furthermore, an experiment carried out without iron but with hydrogen contents equivalent to that produced by corrosion of the iron foil did not show inhibition of the dissolution. This experiment, which is not part of this project, shows that under the experimental conditions of our study, iron is the main active redox species.

This concentration is in agreement with the solubility of amorphous $\text{UO}_2 \cdot x\text{H}_2\text{O}$, thus indicating a thermodynamic equilibrium and not an oxidative dissolution. The total mass balance of uranium indicates that it is mainly sorbed or precipitated on the TiO_2 liner or on the iron foil, with a very low total released of $0.8 \mu\text{g}$.

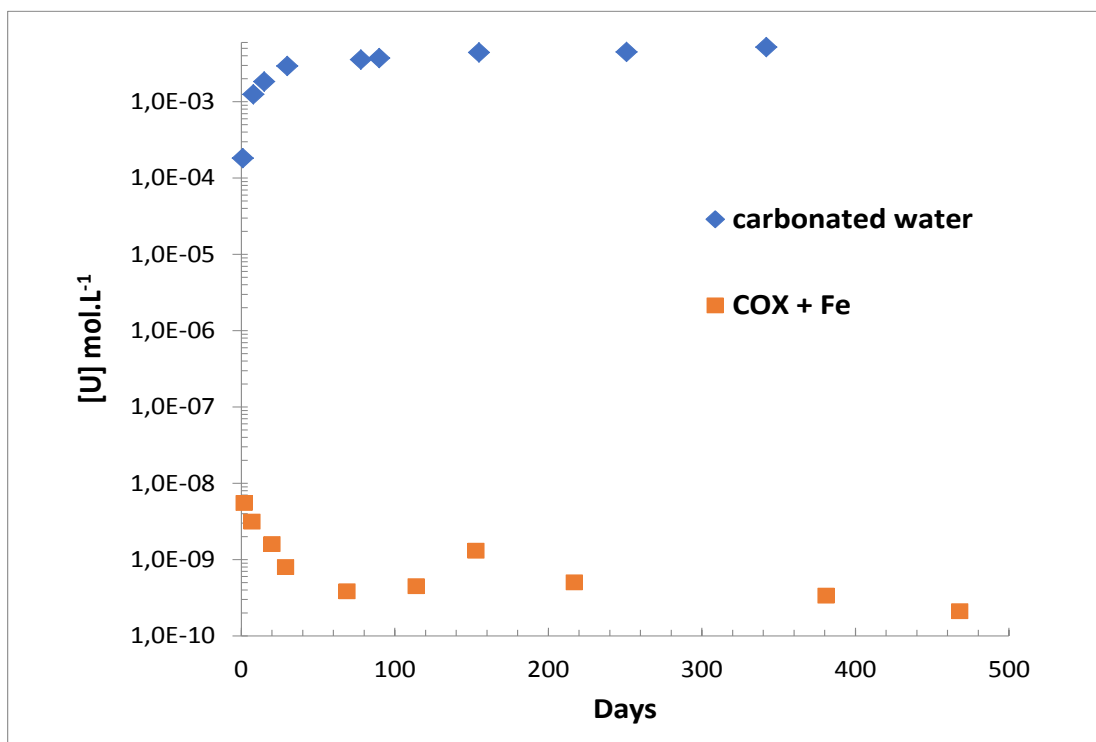


Figure 2.2.1.2: Evolution of uranium concentrations over time (468 days). Carbonated water is a reference to illustrate the major role of iron on the drop in concentrations.

Characterization of the surface of the MOX pellets and of the iron foil was carried out after the leaching experiment: SEM imaging coupled with elemental analyses (EDS) and Raman spectroscopy. The results of these analyses are presented below, first with the characterization of the homogeneous MOX pellet, followed by the characterization of the iron foil.

The pictures obtained by SEM (Figure 2.2.1.3) made it possible to demonstrate massive precipitation on the surface of the MOX fuel pellets. This layer, with a thickness estimated at 26 μm , seems to be made up of a set of interlaced sheets, these sheets themselves being formed of balls. The surface does not seem entirely covered by this precipitate, but it is possible that the handling of the pellet resulted in the partial removal of the deposit.

Elemental analyses (Figure 2.2.1.4) show that this phase is mainly composed of iron and silicon ($\sim 3\%$). Uranium and plutonium are sometimes also detected during elemental analyses, which may be due to a contribution from the underlying MOX matrix, or to sorption / coprecipitation mechanisms on iron.

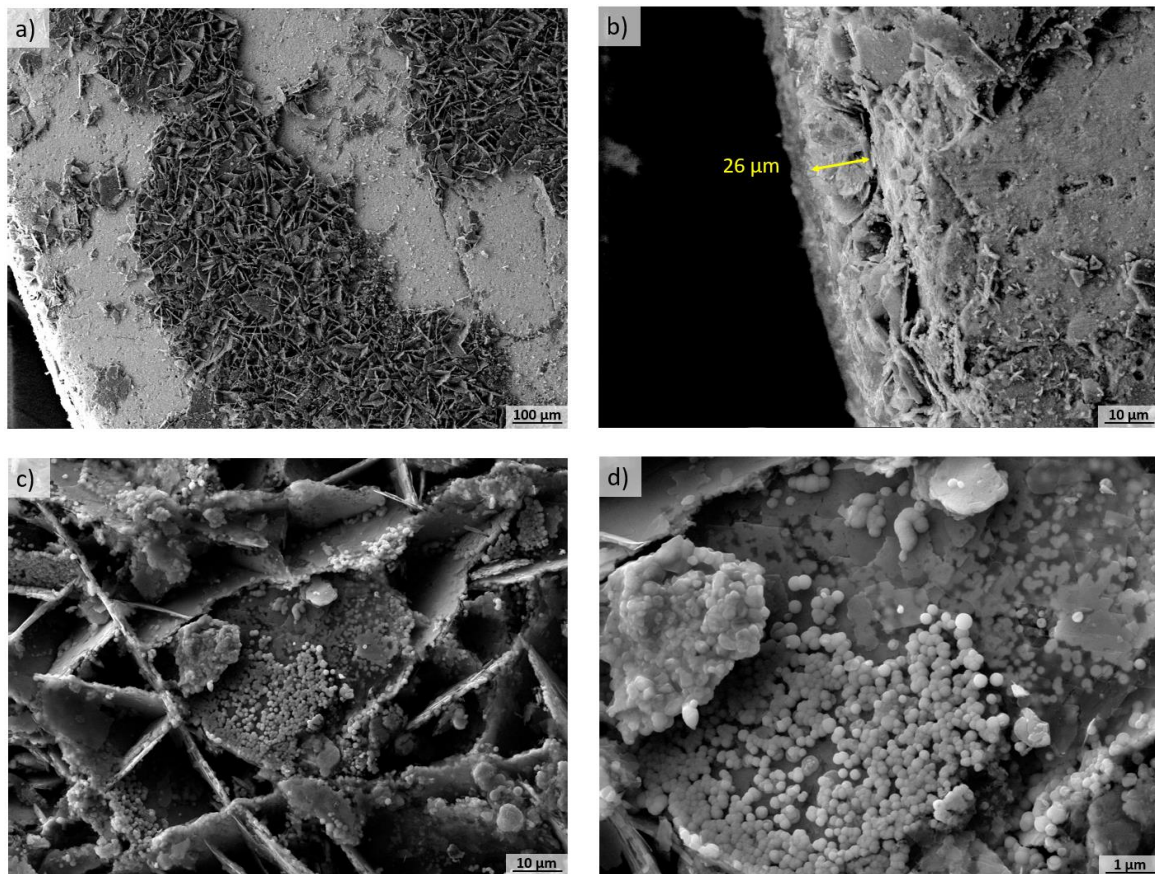


Figure 2.2.1.3: SEM observations of the surface of the MOX pellet after one year of leaching in a synthetic CO_x groundwater and in the presence of a corroded iron foil.

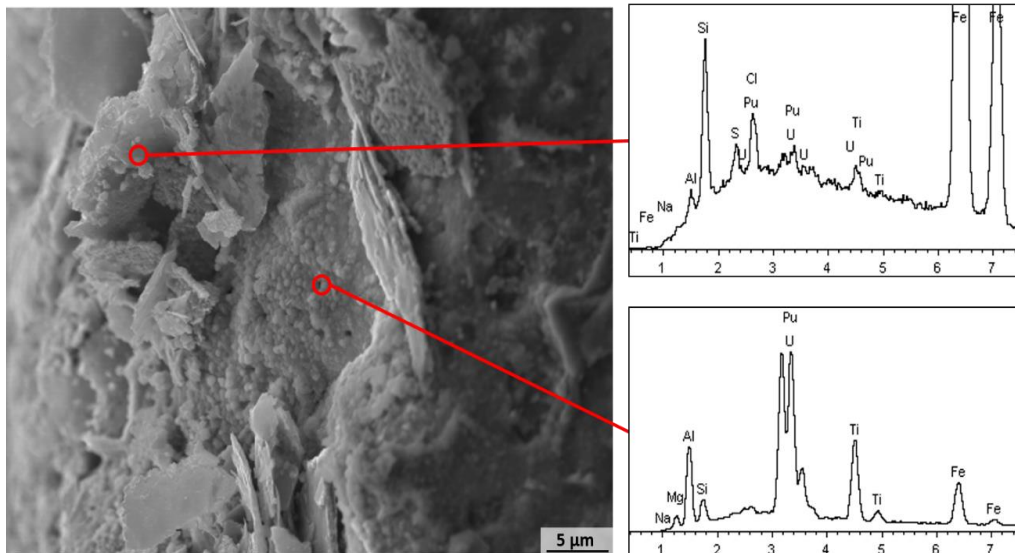


Figure 2.2.1.4: SEM observations and EDS spectrum obtained on the surface of the MOX pellet after one year of leaching. The analysis confirms the presence of iron plates.

In order to determine the nature of the phase observed, analyses by Raman spectroscopy were also carried out. In order not to alter the phase, the first spectra were acquired at low laser power. Subsequently, a study was conducted to choose the optimal working power, that is to say the maximum usable power without altering the sample. Several spectra have therefore been acquired by increasing the power of the beam. At low power (0.12 mW), the spectrum obtained corresponds to that of magnetite (Figure 2.2.1.5).

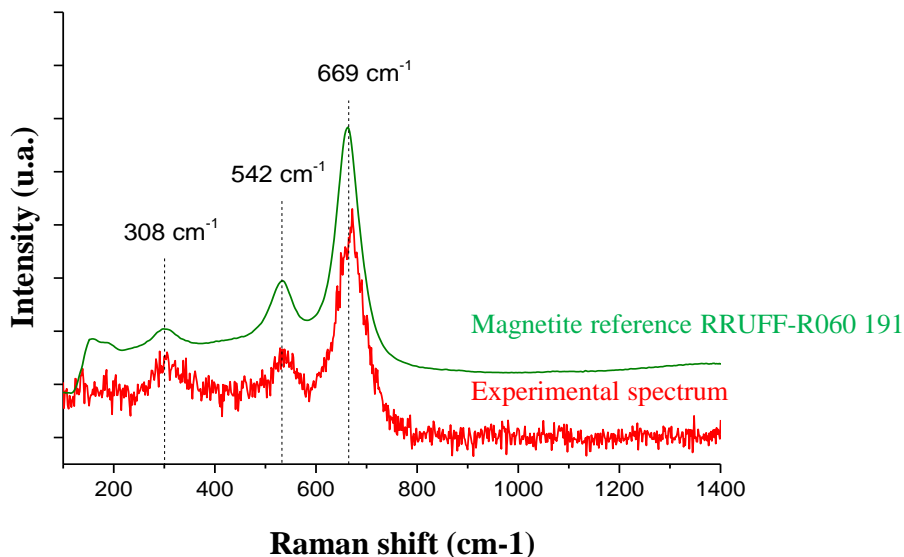


Figure 2.2.1.5: Raman spectrum of magnetite obtained on the surface of the MOX fuel pellet.

SEM images of the surface of the iron foil, shown in Figure 2.2.1.6, show a strong precipitation of secondary phases. Two kinds of phases can be observed: needles and balls / sheets. Elemental analyses show that the needles are mainly composed of calcium with low

strontium contents. These results are in agreement with the drop in calcium and strontium concentrations in solution mentioned before. The balls of sheets, on the other hand, are mainly composed of iron.

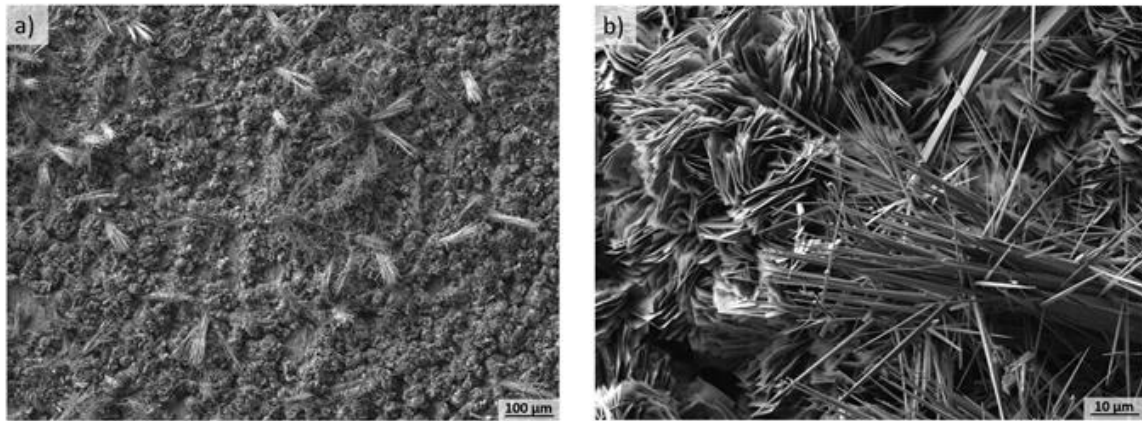


Figure 2.2.1.6: SEM observations of the surface of the iron foil after 552 days of leaching in synthetic CO_x groundwater.

In order to identify the phases observed, Raman analyses were carried out. The power was initially adjusted to 0.29 mW in order not to alter the phases. Two different spectra have been collected on the surface of the iron blade: the chukanovite spectrum and the aragonite spectrum (Figure 2.2.1.7). Aragonite corresponds to the needles observed on the surface by SEM. The iron balls correspond to chukanovite, the morphology observed being similar to that observed elsewhere in the literature [18]. Other elements are also present, including sulphur, magnesium, chlorine and silicon, which can promote the precipitation of aragonite and chukanovite at the expense of calcite and siderite.

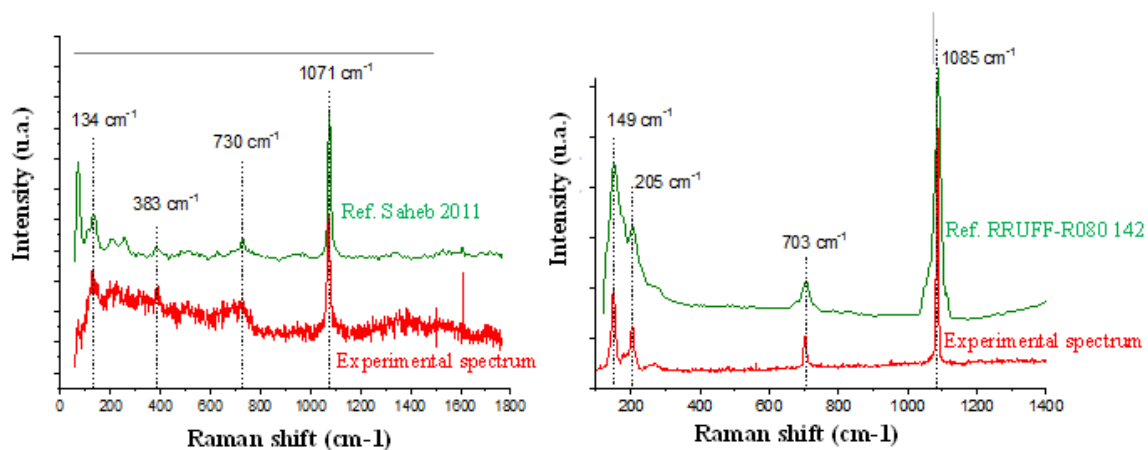


Figure 2.2.1.7: Raman spectra of chukanovite (left) and aragonite (right) obtained on the surface of the iron foil.

Aragonite is a polymorph of calcite and several studies show that it is favoured in environments rich in magnesium, which is the case for CO_x groundwater. Furthermore, it is interesting to note that aragonite tends to transform into calcite under the effect of

temperature, thus indicating that aragonite is metastable and evolves into calcite. Similarly, by studying the superposition of Pourbaix diagrams of siderite and chukanovite produced by Azoulay et al. [19] it appears that the stability domain of chukanovite is entirely included in that of siderite. This indicates that chukanovite is metastable, probably evolving into siderite in the long term.

Dissolution mechanisms – Fe(II) released in solution by the iron foil anoxic corrosion consumes H_2O_2 produced by alpha-radiolysis of water (Figure 2.2.1.8). This redox reaction occurs where radiolytic H_2O_2 is produced, i.e. on the extreme surface of the MOX pellets. The Fe(III) produced precipitates immediately onto the MOX pellets as magnetite. Thanks to this consumption of H_2O_2 , the oxidative dissolution of MOX fuel is strongly inhibited by the presence of metallic iron. It would seem that the location of the redox front on the extreme surface of MOX favours the inhibition of oxidizing dissolution under alpha radiolysis which occurs in the very first microns of the reactional interface. In parallel, a local increase in pH around the iron foil due to its anoxic corrosion enables the precipitation of carbonated secondary phases (aragonite, chukanovite) onto its surface.

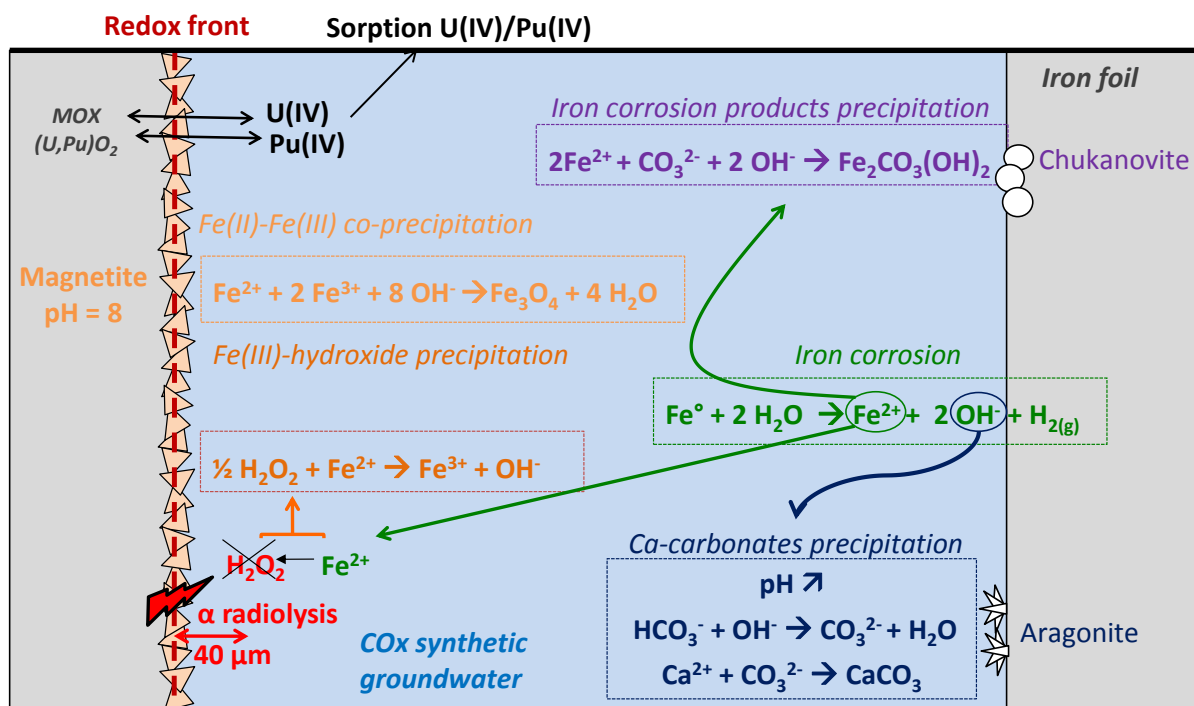


Figure 2.2.1.8: General scheme showing the coupled mechanisms of dissolution of a homogeneous MOX fuel in a synthetic CO_x groundwater and in the presence of an iron foil.

These mechanisms are very similar to those observed on UO_x type fuels. However in previous work [18], magnetite had not been observed on the surface of the fuel pellets but rather iron hydroxides like akaganeite. The slightly more basic pH measured for the MOX experiment seems able to explain these differences in the iron-based phases formed. Finally, all of this data is the subject of modelling work in the context of DisCo WP5.

3 Concluding perspective

This report summarizes the preliminary results of dissolution experiments on Cr/Al/Gd-doped-UO₂-based and MOX model systems performed by DisCo WP4 participants available as of May 2020 – final results will be available at the end of the DisCo project. In particular, this report provides the modellers from WP5 with detailed information from the various groups involved in WP4 on the pellets used in the experiments, the experimental conditions, and the experimental observations in a structured and coherent way by using an electronic exchange format. Thus this deliverable and the electronic data exchange provide a solid basis for future modelling activities within DisCo WP5. The dissolution behaviour of the model systems was studied on pellet samples, which were prepared by the various groups active in WP2 by different approaches. In particular the preparation of the doped UO₂-materials lead to a set of samples, which cover broad ranges in terms of dopant levels/composition and microstructure. Since these parameters are not well known for irradiated modern fuel pellets, the approach followed here ensures that the envelope of these parameters in the model systems covers most likely also those in “real” SNF. Moreover, this range of material properties will aid in elucidating effects of microstructure and dopant concentration and speciation on the dissolution behaviour in single-effect and multi-parametric studies. This will further strengthen the complementary approach followed in DisCo of combining leaching studies on SNF with dissolution studies on model materials for unravelling the long-term corrosion behaviour of conventional and modern SNF in a variety of repository-relevant conditions.

4 References

- [1] Cachoir, C., 2019. Preparation of evolved cement water (ECW, ECW-light), young cement waters (YCW, YCWCa and YCWCa-light) and of cement water (OCW) for the Supercontainer experiments. SCK CEN restricted report SCK CEN/12272337, SCK•CEN, Mol, Belgium.
- [2] Farnan, I., Bosbach, D., Wegen, D., Gonzales-Robles Corrales, E., Jegou, C., Corkhill, C., Hambley, D.I., Cobos Sabate, J., 2018. WP2-Initial state report: sample characterisation and experimental set-up. Deliverable D2.1 of the European DisCo project.
- [3] Delville, R., 2019. Investigation of fabrication routes of model fuels with tailored microstructures for leaching studies. 30th Spent Fuel Workshop, November 14-15, 2019, Ghent, Belgium.
- [4] Cachoir, C., Mennecart, T., Lemmens, K., 2019. Dissolution experiments with Cr-(Pu) doped UO₂ at FZJ and SCK CEN: Preparatory tests with depleted and low alpha-doped UO₂ at SCK CEN. 2nd Annual Meeting of the European DisCo project, May 27-28, 2019, Cologne, Germany.
- [5] Bosbach, D., Cachoir, C., Myllykylä, E., Jegou, C., Cobos, J., Farnan, I., Corkhill, C., 2019. WP4-model materials experiments: First dissolution results. Deliverable D4.1 of the European DisCo project.
- [6] Neck, V., Kim, J.I., 2001. Solubility and hydrolysis of trivalent actinides. *Radiochimica Acta* 89, 1-16.
- [7] Ekeröth, E., Jonsson, M., 2003. Oxidation of UO₂ by radiolytic oxidants. *Journal of Nuclear Materials* 322, 242-248.
- [8] Maier, A.C., Kegler, P., Klinkenberg, M., Baena, A., Finkeldei, S., Brandt, F., Jonsson, M., 2020. On the change in UO₂ redox reactivity as a function of H₂O₂ exposure. *Dalton Transactions* 49, 1241-1248.
- [9] Ollila, K., Albinsson, Y., Oversby, V., Cowper, M., 2003. Dissolution rates of unirradiated UO₂, UO₂ doped with ²³³U, and spent fuel under normal atmospheric conditions and under reducing conditions using an isotope dilution method. SKB Technical Report TR-03-13, Svensk Kärnbränslehantering AB, Stockholm, Sweden.
- [10] Ollila, K., Oversby, V., 2004. Measurement of dissolution rates of UO₂ matrix with the isotope dilution method. *Materials Research Society Symposium Proceedings* 807, 47-52.
- [11] Ollila, K., Oversby, V., 2005. Dissolution of unirradiated UO₂ and UO₂ doped with ²³³U under reducing conditions. Posiva Report 2005-05, Posiva Oy, Olkiluoto, Finland.
- [12] Ollila, K., 2008. Dissolution of unirradiated UO₂ and UO₂ doped with ²³³U in low- and high-ionic strength NaCl under anoxic and reducing conditions. Posiva Working Report 2008-50, Posiva Oy, Olkiluoto, Finland.
- [13] Zetterström Evins, L., Juhola, P., Vähänen, M., 2014. REDUPP Final Report (FP7, agreement no. 269903). Posiva Working Report 2014-12, Posiva Oy, Olkiluoto, Finland.
- [14] Ollila, K., Myllykylä, E., Tanhua-Tyrkkö, M., Lavonen, T., 2013. Dissolution rate of alpha-doped UO₂ in natural groundwater, *Journal of Nuclear Materials* 442, 320-325.

- [15] Yajima, T., Kawamura, Y., Ueda, S., 1995. Uranium(IV) solubility and hydrolysis constants under reduced conditions. Materials Research Society Symposium Proceedings 353, 1137-1142.
- [16] Ollila, K., 2008. Solubility of UO_2 in the high pH range in 0.01 to 0.1 M NaCl solution under reducing conditions. Posiva Working Report 2008-75, Posiva Oy, Olkiluoto, Finland.
- [17] Gimenez, J., Clarens, F., Casas, I., Rovira, M., de Pablo, J., Bruno, J., 2005. Oxidation and dissolution of UO_2 in bicarbonate media: Implications for the spent nuclear fuel oxidative dissolution mechanism. Journal of Nuclear Materials 345, 232-238.
- [18] Odorowski, M., Jegou, C., De Windt, L., Broudic, V., Jouan, G., Peugeot, S., Martin, C., 2017. Effect of metallic iron on the oxidative dissolution of UO_2 doped with a radioactive alpha emitter in synthetic Callovian-Oxfordian groundwater. Geochimica Cosmochimica Acta 219, 1-21.
- [19] Azoulay, I., Rémazeilles, C., Refait, P., 2012. Determination of standard Gibbs free energy of formation of chukanovite and Pourbaix diagrams of iron in carbonated media. Corrosion Science 58, 229-236.

Acknowledgement

The research leading to these results has received funding from the European Commission Horizon 2020 Research and Training Programme of the European Atomic Energy Community (EURATOM) (H2020-NFRP-2016-2017-1) under grant agreement n° 755443 (DisCo project).

Appendix

Database_DISCO_sent-to-ExCom-09062020.xlsx

Sheet Summary Table

	A	B	C	D	E	F	G	H
1	System type							
2	Institution	contact person (email)	Experiment ID #	Solid material (Fuel)	specify if you have answered "other" in column D	Cooling time (for SF)	is sample pre-oxidized?	sample pre-treatment (if applicable) please comment
3								
4								
5								
6								
7								
8								
9								
10								

I	J	K	L	M	N	O	P	Q	R	S	T	U	V	W	X	Y
Solid material type																
FGR INFO	Alpha/ Beta Activity (MBq/g)	Cr/Al/RE/ α Dopant	is doping homogeneous?	% Dopant (molar or weight)	Sample Preparation	specify if you answered "other" in column K	Sample Type	specify if you answered "other" in column M	with cladding? (Y/N)	BU(GWd/tHM) Average or Local (specify)	Reactor Type	Initial fuel enrichment	Linear power (W/cm) Average or Local (specify)	Cladding	Region sampled	Sample size

Z	AA	AB	AC	AD	AE	AF	AG	AH	AI	AJ	AK	AL	AM	AN	AO	AP
Solid Characterization			Experimental Conditions													
BET / Geometrical SA	Grains diametre (μ m)	Porosity	Site Density (mol sites/m ²)	Total Reaction Time (days)	Sample Weigth (g)	Solution Volume (L)	T (°C)	% composition of the contacting gas phase	Fe(s) addition	type of Solution System	Specify if you answered "other" in column AF	Solid characterization techniques	Solution analysis techniques	Gas analysis techniques	Ref. publicaiton	Year Publication

Sheet Experiment#1

	A	B	C	D	E	F	G	H	I	J	K	L	M	N	O	P	Q	R	S	T	U	V	W
1																							
2																							
3	Sample	Reaction Time (days)	FGR (%)	pH	Eh (V)	[Na] (M)	[K] (M)	[Mg] (M)	[Ca] (M)	[Sr] (M)	[Si] (M)	[C(in)] (M) or pCO2 (bar)	[C(org)] (M)	[S(6)] (M)	[S(-2)] (M)	[Cl(-1)] (M)	[Cl(+7)] (M)	[Br(-1)] (M)	[F(-1)] (M)	[N(+3)] (M)	[N(+5)] (M)	[H2O2] (M)	[P(+5)] (M)
4	initial	0																					
5	t1																						
6	t2																						
7	t3																						
8																							
9																							
10																							

X	Y	Z	AA	AB	AC	AD	AE	AF	AG	AH	AI	AJ	AK	AL	AM	AN	AO	AP	AQ	AR	AS	AT
[OH-] (M)	[O2] (M) or pO2(bar)	[H2] (M) or pH2 (bar)	[Cr] (M)	[Al] (M)	[Ba] (M)	[Gd] (M)	[Th] (M)	[Fe] (M)	[Mn] (M)	[U] (M)	[Pu] (M)	[Np] (M)	[Am] (M)	[Cm] (M)	[Tc] (M)	[Sr] (M)	[Mo] (M)	[Zr] (M)	[Rb] (M)	[Se] (M)	[Cs] (M)	[I] (M)

AV	AW	AX	AY	AZ	BA	BB
BET / Geometrical SA (m2/g)	Grains size (µm)	Porosity	Comments (alteration layer?, secondary phases formed?) Please comment	add new columns if needed		